University of Maribor
Faculty of Energy Technology

Journal of ENERGY TECHNOLOGY

Volume 13 / Issue 2
SEPTEMBER 2020
www.fe.um.si/en/jet.html

Journal of ENERGY TECHNOLOGY

VOLUME 13 / Issue 2

Revija Journal of Energy Technology (JET) je indeksirana v bazah INSPEC© in Proquest's Technology Research Database.

The Journal of Energy Technology (JET) is indexed and abstracted in database INSPEC© and Proquest's Technology Research Database.

JOURNAL OF ENERGY TECHNOLOGY

Tehnični urednik / TECHNICAL EDITOR

Sonja Novak

Tehnična podpora / TECHNICAL SUPPORT

Tamara BREČKO BOGOVČIČ

Izhajanje revije / PUBLISHING

Revija izhaja štirikrat letno v nakladi 100 izvodov. Članki so dostopni na spletni strani revije - www.fe.um.si/si/jet.html / The journal is published four times a year. Articles are available at the journal's home page - www.fe.um.si/en/jet.html.

Cena posameznega izvoda revije (brez DDV) / Price per issue (VAT not included in price): 50,00 EUR

Informacije o naročninah / Subscription information: http://www.fe.um.si/en/jet/subscriptions.html

Lektoriranje / LANGUAGE EDITING

Terry T. JACKSON

Oblikovanje in tisk / DESIGN AND PRINT

Fotografika, Boštjan Colarič s.p.

Naslovna fotografija / COVER PHOTOGRAPH

Jurij AVSEC

Oblikovanje znaka revije / JOURNAL AND LOGO DESIGN

Andrej PREDIN

Ustanovni urednik / FOUNDING EDITOR

Andrej PREDIN

Spoštovani bralci revije Journal of energy technology (JET)

V Sloveniji predstavljajo termoenenergetski procesi zelo pomemben delež k pridobivanju toplotne in električne energije, kakor tudi v pogonih avtomobilov, tovornjakov in ladij. Eden pomembnejših termoenergetskih procesov v sodobnih termo in jedrskih elektrarnah je Rankinov proces v vseh njegovih variacijah. Avtor Rankinovega procesa je škotski termodinamik William J.M. Rankine (1820-1872), ki je ta proces objavil leta 1859.

V zadnjem času se kaže v svetu velik napredek v aplikaciji vodikovih tehnologij. Pričakuje se, da bodo cene vodika v prihodnjih letih drastično upadle, kot so pričele padati tudi cene gorivnih celic. Trenutna številka revije JET prikazuje idejo masovnega pridobivanja vodika s pomočjo soproizvodnje električne energije, toplotne energije in vodika v Rankinovem procesu. Zaradi ekoloških dejavnikov ter dejstva, da bo klasičnih virov v bližnji prihodnosti zmanjkalo, je velikega pomena izkoriščanje obnovljivih virov energije.

V tej številki revije JET je prikazana tudi ideja proizvodnje toplotne energije s pomočjo sonca v sončnih kolektorjih. V ta namen je raziskana analiza življenjskega cikla sončnih kolektorjev. Analiza življenjskega cikla daje zelo natančen vpogled o dejanski uporabnosti in ekološki sprejemljivosti energetskih naprav.

Vsem bralcem želim obilo zanimivega branja.

Jurij AVSEC
odgovorni urednik revije JET

Dear Readers of the Journal of Energy Technology (JET)

In Slovenia, thermal energy processes represent a crucial share in the production of thermal energy, electricity as well as in the power processes of cars, trucks and ships. One of the most important thermal energy processes in modern thermal and nuclear power plants is the Rankine process in all its variations. The process is named after the Scottish thermodynamicist William J.M. Rankine (1820–1872), who published this process in 1859.

Recently, the world has shown great progress in the application of hydrogen technologies. Hydrogen prices are expected to fall drastically in the coming years, and fuel cell prices have also started to decline. The present issue of JET magazine discusses the idea of mass production of hydrogen through the cogeneration of electricity, heat, and hydrogen in the Rankine process. Due to ecological factors and the fact that conventional resources will run out in the near future, the use of renewable energy sources is of great importance.

The current issue presents the idea of producing thermal energy with the help of the sun in solar collectors. To this end, a life cycle analysis of solar collectors is investigated. A life cycle analysis of each energy device on the actual usability and ecological acceptability of energy devices is conducted.

I wish all readers plenty of interesting reading

Jurij AVSEC
Editor-in-chief of JET

Table of Contents / Kazalo

Journal of Energy Technology

JET Volume 13 (2020) p.p. 11-26
Issue 2, September 2020
Type of article 1.01
www.fe.um.si/en/jet.html

MULTI-PURPOSE USE AND LIFECYCLE ANALYSIS OF SOLAR PANELS

VEČNAMENSKA UPORABA IN ANALIZA ŽIVLJENJSKEGA CIKLA SOLARNEGA PANELA

Dušan Strušnik[1], Urška Novosel[2], Jurij Avsec[✉]

Keywords: heat pump, life cycle analysis, Rankine cycle, solar panel, thermochemical cycle

Abstract

The combined use of renewable energy technologies and alternative energy technologies is a promising approach to reduce global warming effects throughout the world. In this paper, the solar panel is used in combination with a heat pump or with biomass sources to obtain heat, electricity, and hydrogen. Based on the Rankine thermodynamic cycle, hydrogen could be obtained from water with electrolysis and the CuCl thermochemical cycle. Furthermore, this study contains a life cycle analysis of solar panels.

Povzetek

Kombinirana uporaba tehnologij obnovljivih virov energije in tehnologij alternativnih energij je obetaven pristop za zmanjšanje učinkov globalnega segrevanja v svetu. V tem prispevku se sončna plošča uporablja v kombinaciji s toplotno črpalko ali z viri biomase za pridobivanje toplote, električne energije in vodika. Na podlagi Rankinovega termodinamičnega cikla bi lahko s pomočjo CuCl termokemičnim ciklom iz vode pridobivali tudi vodik. Poleg tega študija prikazuje analizo življenjskega cikla solarnega panela.

[✉] Corresponding author: Dušan Strušnik, Energetika Ljubljana d.o.o., TE-TOL Unit, Toplarniška 19, 1000 Ljubljana, E-mail address: dusan.strusnik@gmail.com

[1] Energetika Ljubljana d.o.o., TE-TOL Unit, Toplarniška 19, SI-1000 Ljubljana, Slovenija

[2] University of Maribor, Faculty of Energy Technology, Hočevarjev trg 1, SI-8270 Krško, Slovenia

1 INTRODUCTION

The production of electricity and heat from renewable sources is becoming more efficient and economically viable. Given current environmental problems, the utilization of renewable energy sources is becoming desirable. The demand for thermal energy accounts for more than half of the world's total energy needs. Currently, most of that heat is generated from hydrocarbons and their derivatives. Some small amounts are produced through renewable energy sources throughout the world. In the future, it is expected that the production of heat from renewable sources will significantly exceed the current level. For this purpose, all types of renewable energy sources should be taken into account. Particularly interesting is the use of solar energy with solar collectors, which have a yield of over 60%, *[1].* Currently, there are several solar thermal generation systems, including plate collectors, vacuum collectors, and hot-air collectors, with which solar and thermal energy can be simultaneously obtained. In the foreground, there are also solar panels, which can be used in different ways: mounted on the roof, to cover the facades of houses, and similar. In this way, they could acquire a good portion of the energy required for home and industrial heating. Fig. 1 shows a wall mounting and a roof mounting of a solar panel with aluminium tubes and rock wool insulation material.

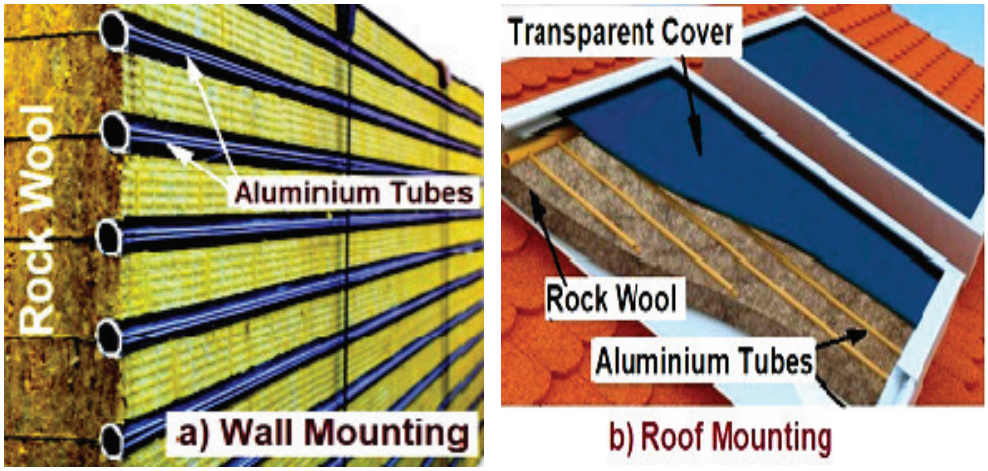

Figure 1: a) *a wall mounting solar panel and b) a roof mounting solar panel*

In this case, the solar panel is comprised of aluminium tubes, rock wool insulation material, transparent cover, circulation pump, etc. The panels are usually roof-mounted; however, they can also be mounted on the building walls or on frames on the ground.

The insulator located between represents the thermal building envelope and should keep heat losses as low as possible. If the solar panel is mounted in the wall, rock wool represents the thermal building envelope. Due to this sophisticated revision of sandwich panels, the field of application can be extended to office buildings, residential buildings, public buildings (e.g., education, culture, health, etc.).

2 SOLAR PANEL MULTI-PURPOSE USE ANALYSIS

2.1 The solar panel as a hydrogen producer

The main idea of the present article is the use of solar energy and biomass (wood chips) to produce cheap hydrogen. We combined two processes for hydrogen production: electrolysis and the thermochemical CuCl cycle. The working Rankine cycle system combined with the CuCl process, *[2]*, and the electrolysis system is presented in Fig. 2 and Fig. 3.

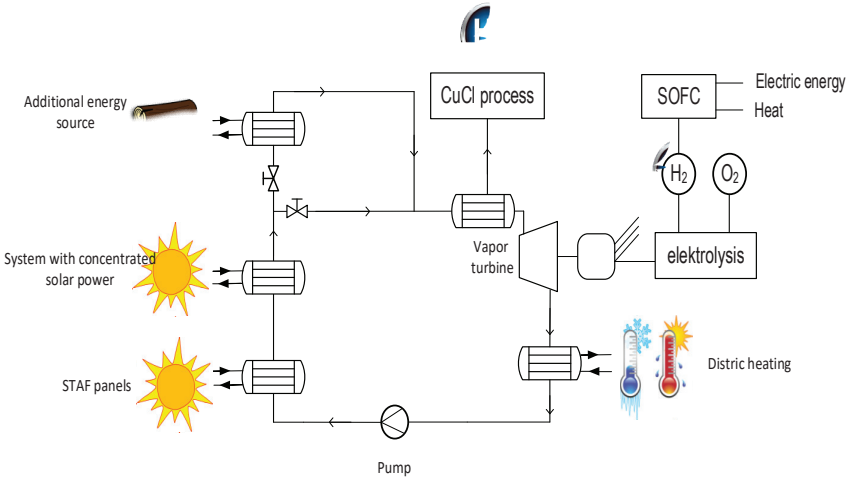

Figure 2: Solar panels in combination with Rankine cycle

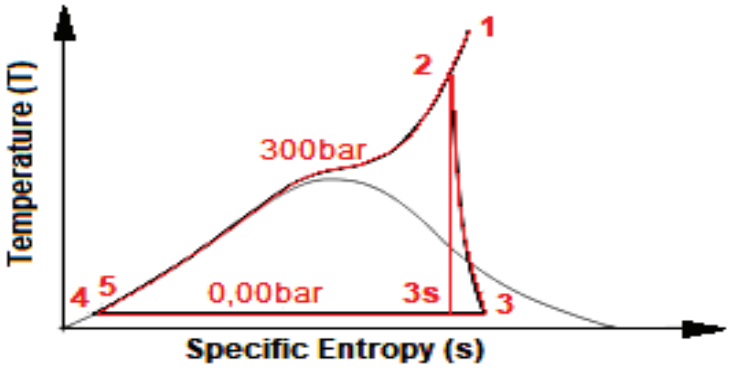

Figure 3: T-s diagram of the Rankine cycle

Apart from hydrogen production in the process, we can also use waste heat from the Rankine cycle for district low-temperature heating of buildings and houses. All necessary data to calculate thermodynamic efficiency are presented in Table 1.

Table 1: *Results of the Rankine system calculation*

Rankine system and CuCl system		
State	***Pressure [bar]***	***Enthalpy [kJ/kg]***
1	300	3883.43
2	300	3599.4
3s	0.06	1972.8
3	0.06	2135.46
4	0.06	151.5
5	300	186.765
Parameter	***Value***	
$\dot{W}_T$	10 MW	
η_s	0.9	
$\dot{m}_1$	6.831 kg/s	
$\dot{Q}_4$	–13.552 MW	
$\dot{m}_{sw}$	403.346 kg/s, ΔT = 8 K	
$\dot{W}_p$	240.9 kW	
η_p	0.85	
Q_{solid}	25.252 MW	
$\dot{W}_{CuCl}$	1.94 MW	

This relatively small cogeneration unit was built for the Posavje region of Slovenia. The idea of the present work is primarily to exploit solar energy for hydrogen production. Large amounts of solar energy are available, especially in the summer, spring, and autumn. To this end, we have used a model of covered solar panels, with which we could obtain approximately 20 °C of temperature increase. Additional heat for the processes is obtained from wood chips. With the help of solar calculation software found on the web page "The European Commission's science and knowledge service", *[3]*, we have calculated the average amount of solar hours. For solar panels integrated into building for Posavje region, we calculated 1060 effective solar hours for solar angle 450 and 716 effective solar hours for solar angle 900.

Fig. 4 shows the production of hydrogen per day with the Rankine cycle system, electrolysis and CuCl system. On the basis of thermodynamic calculation, we could determine the amount of hydrogen produced by the CuCl process and by electrolysis per day. As seen in Fig. 4, the total production of hydrogen is 3931.5 kg/day; the ratio between the hydrogen obtained by electrolysis and the CuCl process is more than 5.

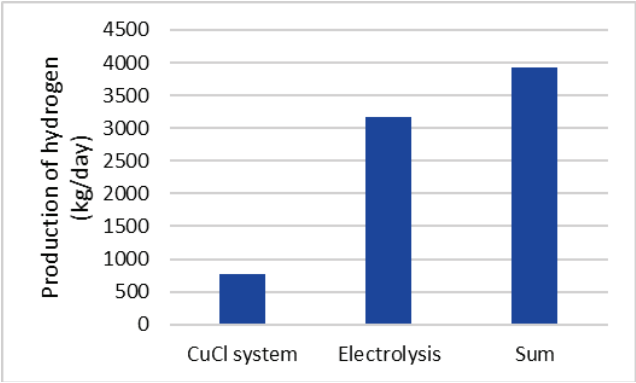

Figure 4: The amount of produced hydrogen

2.2 The solar panel as a cooling system

The use of thermal energy produced by a solar panel for cooling processes is also extremely interesting from a technical point of view. For this purpose, two cooling systems are presented. The first system represents cooling by means of an absorption refrigeration device and solar panels (Fig. 5). The second system represents cooling by means of solar panels, the ORC system and compressor heat pump (Fig. 6).

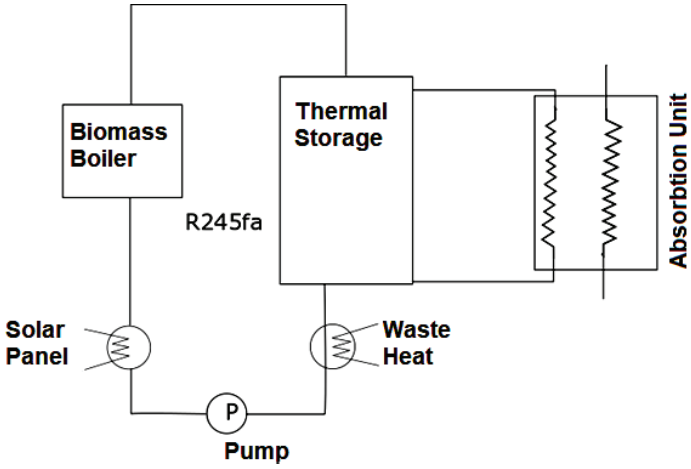

Figure 5: Cooling by means of an absorption cooling device and solar panel

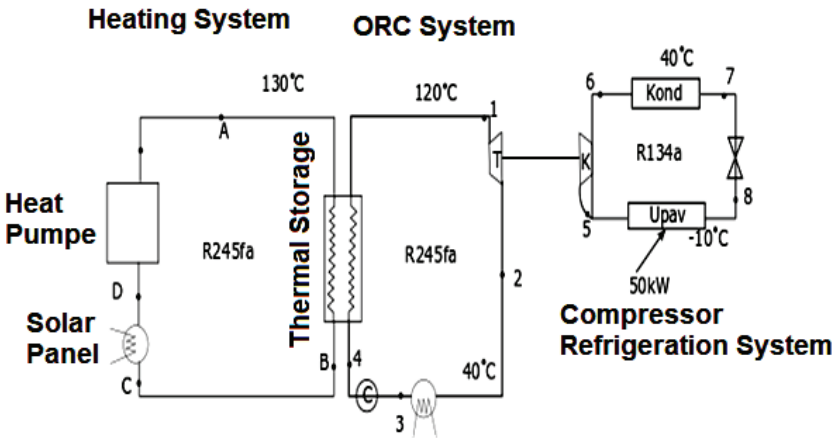

Figure 6: Cooling by means of solar panel, ORC system and compressor heat pump

3 LIFE CYCLE ANALYSIS OF SOLAR PANEL

Life cycle analysis is a tool for assessing the energy and environmental profile of a product or technology from design to recycling. It provides global guidance and criteria, based on which decisions are made on further product development and which accompany the product or technology throughout the life cycle. Life cycle analysis covers the entire energy and environmental aspect from production, transport, installation, lifetime and decommissioning of a product. It is a methodology that includes four life cycle phases in a comprehensive and transparent way, on the basis of facts and expertise and in conformity with the ISO 14040 standard *[4]*. These phases are study goal and scope definition, data acquisition, modelling and interpretation of results. As regards new process and product development, the relationship between processes, product characteristics and environmental impacts have to be taken into consideration for each product. The international ISO 14025 standard, *[5]*, was introduced to ensure comparable environmental efficiency among products. The main stages of life cycle analysis are presented in Fig. 7.

Figure 7: Main stages of life cycle analysis

The life cycle analysis of solar panels comprises several phases, and each phase covers input-output data on materials, energies and environmental impact factors. Other authors developed life cycle analysis in a similar way, *[6]*, *[7].* In the solar panel production phase, the life cycle analysis includes extraction, production and transformation of raw materials required for the manufacture of a solar panel first as a semi-finished product, then as a product and finally an end product. The phase of a life cycle analysis involving solar panel production comprises three steps: material production, product manufacturing, packaging, and distribution. The phase of a life cycle analysis involving the solar panel application includes installation, use, and maintenance of a solar panel. The phase of a life cycle analysis involving recycling and waste management includes energy consumption for solar panel recycling and waste management. The environmental factor assessing the environmental burden accompanies all life cycle stages. The life cycle analysis model of a solar panel comprises input-output data and system boundaries. The input data relates to the data on raw materials, energy and hazardous waste used for solar panel manufacture. The output data relates to air emissions, aqueous waste, solid waste, energy, recycled material, and other products. The air emission data includes the data on produced or reduced greenhouse gases of the solar panel life cycle. Aqueous waste affects water management due to its discharge into the environment and the related environmental impacts in the solar panel life cycle. Solid waste is waste generated in the solar panel life cycle without the possibility of recycling. The energy on the output data side constitutes the solar panel energy life cycle and is the ratio between the energy invested, required for the solar panel production, and energy generated by the solar panel in its life cycle. Recycled material is material that can be reprocessed or reused in any other way and has been used in the solar panel life cycle. Other products are undefined products, occurring in the solar panel life cycle. A schematic arrangement of the analysis model of the solar panel life cycle is presented in Fig. 8.

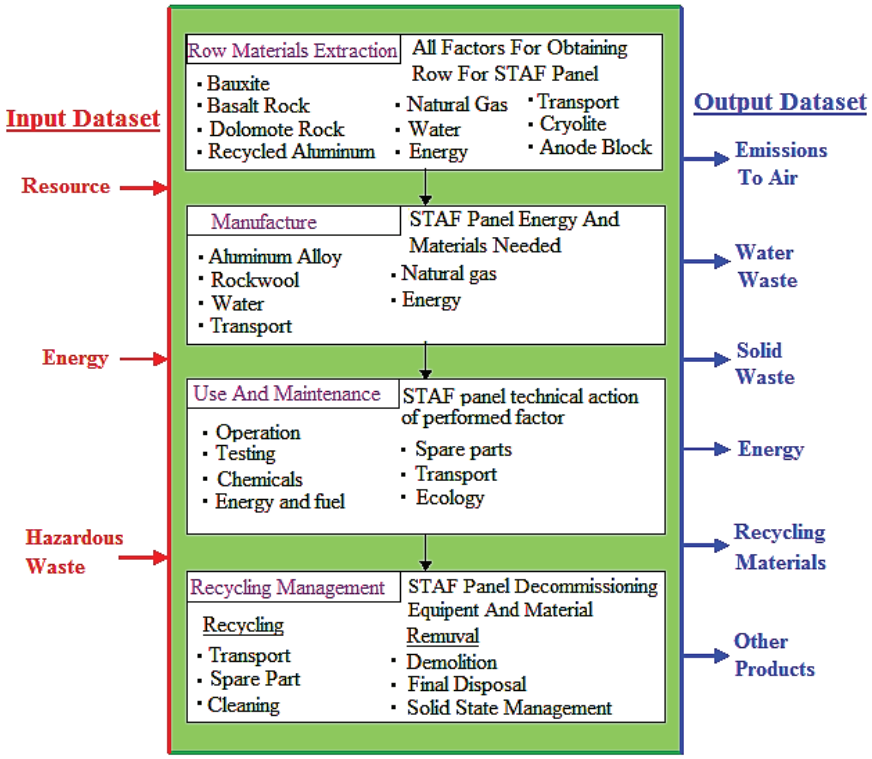

Figure 8: Schematic arrangement of solar panel life cycle analysis model

The quality of a life cycle analysis largely depends on the accuracy and precision of data and databases used. As a result of technological progress and increasingly stringent environmental regulations, the data and databases are constantly subject to changes and updates. The data from various databases differ because they are subject to various regional environmental regulations. The source of primary data in the life cycle analysis of a solar panel was the data provided by the solar panel manufacturer, i.e., Talum, d. d., *[8]*. As a secondary source of data, ee used the databases created by private or academic database developers: Ecoinvent Database, *[9]*, Eurostat, *[10]*, data from scientific literature, *[11]*, *[12]*, data from technical literature, *[13]*, *[14]*, etc. We split the data used in the life cycle analysis model of a solar panel into the following groups: materials, energy, waste, waste heat and air emissions.

3.1 Materials

The materials group contains all materials used in the life cycle analysis model of a solar panel. They were split into two groups, namely aluminium materials for production, installation and packaging of aluminium and materials for production, installation, and packaging of rock wool.

Table 2 shows the database of average quantities of materials used for the solar panel manufacture.

Table 2: *Average quantities of materials for solar panel manufacture*

Aluminium			**Rock wool**		
Material	**kg/panel**	**kg/kg$_{(AL)}$**	**Material**	**kg/panel**	**kg/kg$_{(KV)}$**
Water	1558.336	193.8	Water	-	4.468
Bauxite	39.774	5.100	Bauxite	-	0.086
PE-foil	0.183	0.082	PE-foil	-	0.009
Alumina	14.786	1.910	Briquettes	12.321	1.097
Anode blocks	3.502	0.450	Basalt rock	5.655	0.504
Coke	2.462	0.316	Portland cement	1.158	0.103
Aluminium fluoride	1.362	0.175	Dolomite rock	0.653	0.058
Tar pitch	0.494	0.063	Phenol	0.236	0.021
Green residue	0.045	0.006	Formaldehyde	0.236	0.021
Carbon residue	0.543	0.07	Impregnation	0.022	0.002
Calcium fluoride	0.008	0.001	Iron oxide	0.287	0.025
Cryolite	0.008	0.001	Acrylic dispersion	0.056	0.005
Calcined soda	0.004	0.0005	Total	-	6.399
Total	-	201.974	Total 2	20.624	
Total 1	1621.507				
Total 1+2	1642.131				

As much as 94.9% of water is consumed for the solar panel production, and such water is to a large extent disposed of into the environment as wastewater. The quantity of water required for alumina production is as high as 90%. On average, 39.77 kg of bauxite or 2.4% of the total material consumption is required for the manufacture of one panel. Total consumption of alumina and briquettes amounts to 1.6% of the overall material consumed for the manufacture of a single solar panel. The total quantity of material consumed is 1642.131 kg/panel. The overall amount of the material used for the production of one kilogram of aluminium is 201.974 kg/kg$_{(AL)}$, whereas the overall amount of the material used for the production of one kilogram of rock wool is 6.399 kg/kg$_{(KV)}$.

3.2 Energy

The energy group comprises all energies dealt with in the life cycle analysis model of a solar panel and used in the production or processing stages for the solar panel manufacture. Energy consumed by a solar panel during the one-year or the forty-year operation period and energy generated by the solar panel during the one-year or forty-year operation period is also taken into consideration. In solar panel energy production, the average annual solar radiation for Central Europe [15] is taken into consideration for south-facing orientation and tilt angle of 15°. The energy consumption was split into three groups. We used the consumption of energy per

unit of one kilogram of aluminium for the aluminium production and transport, the energy consumption per unit of one kilogram of rock wool for the production and transport of rock wool and energy consumption per unit of solar panel for the manufacture and transport of solar panels. The one-year and forty-year energy consumption and production for solar panel operation are also included. The database of average energy amounts for the manufacture and operation of solar panels with south orientation and a tilt angle of 15° is shown in Table 3.

Table 3: *Average energy amounts for the manufacture and operation of solar panels with south orientation and a tilt angle of 15°*

Production, process, operation	kWh/kg$_{(AL)}$	kWh/kg$_{(KV)}$	kWh/pan
Primary aluminium	23.99	-	-
Secondary aluminium	2.61	-	-
Briquettes	-	0.579	-
Rock wool	-	1.879	-
Ship transport	0.18	-	-
Rail transport	0.03	-	-
Other transport	0.01	0.024	-
Aluminium panel manufacture	-	-	208.6408
Rock wool production	-	-	26.9895
Assembly and packaging	-	-	1.1772
Recycling	-	-	1.426
Consumption for one-year operation (1)	-	-	251.286
Production – one-year operation (2)	-	-	614.324
Consumption – 40-year operation (3)	-	-	698.616
Production – 40-year operation (4)	-	-	24572.96
Net production – one year (2-1)	-	-	363.038
Net production - 40 years (4-3)	-	-	23874.34

The amount of energy required for primary aluminium production and transport is 23.99 kWh/kg$_{(AL)}$ on average and 2.61 kWh/kg$_{(AL)}$ on average for secondary aluminium production and transport. The ratio between primary and secondary aluminium in the aluminium panel production is 80% to 20%. Rock wool is made from prefabricated briquettes.

The briquette production requires 0.579 kWh/kg$_{(KV)}$ of energy on average, and the rock wool production and transport, however, requires 1.879 kWh/kg$_{(KV)}$ of energy on average. Therefore, the overall energy required for the production and transport of one kilogram of rock wool amounts to 2.388 kWh/kg$_{(KV)}$.

We made a comparison between energy flows of average one-year and 40-year solar panel operation at the average annual solar radiation for Central Europe, south-facing orientation and a tilt angle of 15°. We also took into consideration the average consumption of energy for the operation of a circulating pump that sends a fluid to circulate through the solar panel. The average energy consumption for one-year operation, including the average energy consumption for solar panel manufacture and transport, amounts to 251.286 kWh/panel. In one year, a solar

panel facing south and having a tilt angle of 15°, produces 614.324 kWh/panel on average. Net production in one year is the difference between the average annual energy produced and the average energy consumption for one-year operation, amounting to 363.038 kWh/panel. Furthermore, a similar calculation was made for the 40-year operation. Fig. 9 shows graphical presentations of average energies of the life cycle analysis of a solar panel.

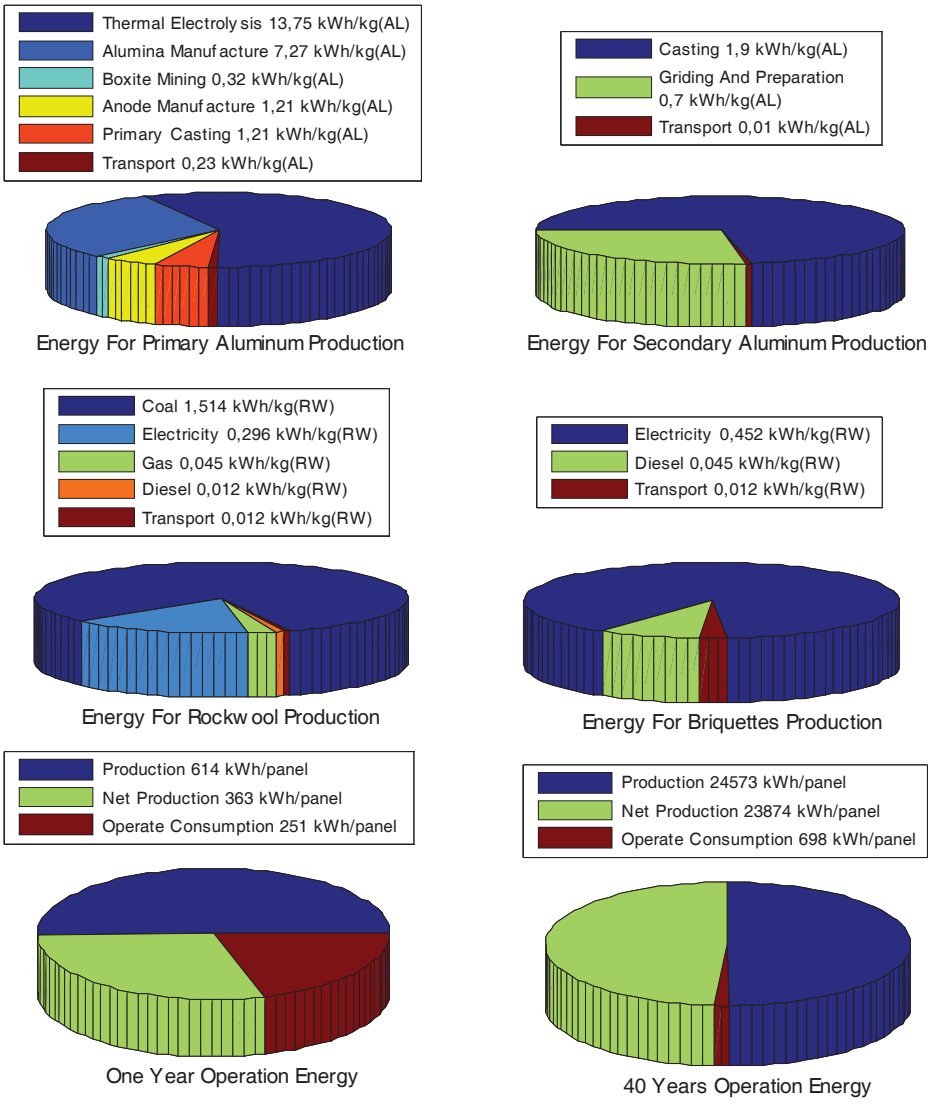

Figure 9: Graphical presentation of average energies of life cycle analysis of a solar panel

Over the one-year period of operation, a solar panel facing south and having at a tilt angle of 15° would produce 2.4 times more energy than the amount required for the manufacture, installation and one-year operation. Over the 40-year period of operation, a solar panel facing south and having a tilt angle of 15° would produce 35 times more thermal energy than the amount required for the manufacture, installation and 40-year operation of a solar panel.

3.3 Air Emissions

In the air emissions group, we used all emissions of CO_2, the greenhouse gas, covered by the model. The CO_2 emissions were split into three groups: emissions in the production and transport of primary raw materials, emissions in the production and transport of rock wool, and emissions in the manufacture and transport of solar panels. The database of average amounts of CO_2 for the manufacture and operation of a solar panel facing south and having a tilt angle of 15° is shown in Table 4.

Table 4: *Average amounts of CO2 for solar panel manufacture and operation*

Production, process, operation	$kg_{(CO2)}/kg_{(AL)}$	$kg_{(CO2)}/kg_{(KV)}$	$kg_{(CO2)}$/panel
Primary aluminium	10.471	-	-
Secondary aluminium	0.8447	-	-
Briquettes	-	0.3734	-
Rock wool	-	0.6181	-
Ship transport	0.0513	-	-
Rail transport	0.0081	-	-
Other transport	0.0027	0.007	-
Aluminium panel manufacture	-	-	83.127
Rock wool production	-	-	10.399
Assembly and packaging	-	-	0.457
Recycling	-	-	0.546
CO_2 production – one-year operation 1	-	-	98.898
CO_2 reduction – one-year operation 2	-	-	226.865
CO_2 production – 40-year operation 3	-	-	277.818
CO_2 reduction – 40-year operation 4	-	-	9074.604
Net reduction of CO_2 – one year (2-1)	-	-	127.97
Net reduction of CO_2 – 40 years (4-3)	-	-	8796.786

The amount of greenhouse gas emissions in the primary aluminium production and transport is 10.471 $kg_{(CO2)}/kg_{(AL)}$ on average and 0,8447 $kg_{(CO2)}/kg_{(AL)}$ on average in the secondary aluminium production and transport. The ratio between primary and secondary aluminium taken into consideration in the aluminium panel manufacture is 80% to 20%.

Rock wool is made of prefabricated briquettes. The amount of greenhouse gas emissions in the briquette production and transport is 0.3734 $kg_{(CO2)}/kg_{(KV)}$ on average and 0,6181 $kg_{(CO2)}/kg_{(KV)}$ on average in the rock wool production and transport. Therefore, the total amount of greenhouse

gas emissions in the production and transport of one kilogram of rock wool is 0.9915 $kg_{(CO2)}/kg_{(KV)}$ on average. Graphical presentation of the average amount of released CO_2 of the life cycle analysis of a solar panel is shown in Fig. 10.

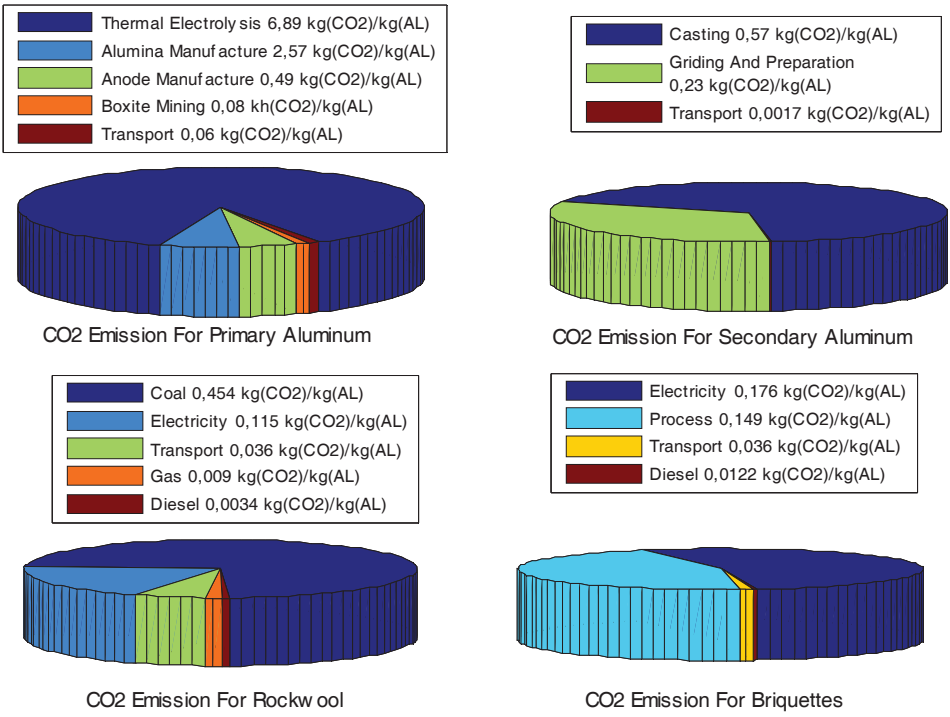

Figure 10: Graphical presentation of the average amount of released CO_2 of the life cycle analysis of a solar panel

3.4 Carbon Footprint

We made a comparison between the carbon footprint of one-year and 40-year operation of a solar panel facing south and having a tilt angle of 15°. All CO_2 gas emissions generated in all stages of solar panel manufacture and transport were taken into consideration in the operation, as well as the greenhouse gas emissions generated in the solar panel operation and circulating pump drive. Those greenhouse gas emissions were reduced by the amount of reduced greenhouse gases to obtain the carbon footprint result in the one-year and 40-year period. Reduced greenhouse gases are gases emitted into the air if the energy generated by a solar panel is produced by burning fossil fuels. The carbon footprint of one-year and 40-year operation of a solar panel facing south and having a tilt angle of 15° is shown in Fig. 11.

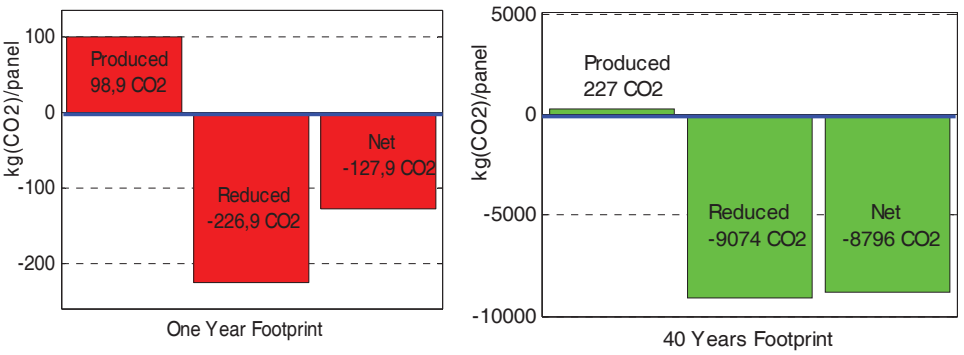

Figure 11: Carbon footprint of one-year and 40-year solar panel operation

Over the one-year period of operation of a solar panel facing south and having a tilt angle of 15°, 98.898 $kg_{(CO2)}$/panel of greenhouse gas are emitted into the air and 226.9 $kg_{(CO2)}$/panel of greenhouse gas are reduced. The one-year carbon footprint is negative, since over the one-year period of a solar panel operation, 127,9 $kg_{(CO2)}$/panel less CO_2 is emitted into the air than if the energy generated by a solar panel in one year is obtained by burning fossil fuels. Over the 40-year period of operation of a solar panel facing south and having a tilt angle of 15°, the amount of CO_2 emitted into the air is 227.818 $kg_{(CO2)}$/panel and the amount of CO_2 reduced is 9074.604 $kg_{(CO2)}$/panel. The 40-year carbon footprint is negative also in this case, since over the 40-year period of a solar panel operation, the amount of CO_2 emitted into the air is by 8796.786 $kg_{(CO2)}$/panel lower than if the energy generated by a solar panel in the period of 40 years is obtained by burning fossil fuels.

4 DISCUSSION AND CONCLUSION

The positive environmental impact of solar panels is reflected mainly in the green production of thermal energy and in its negative carbon footprint. The green production of thermal energy means that solar panels generate 35 times more thermal energy in their life cycle than the energy needed for raw materials production, manufacture, installation and transport of solar panels. The negative carbon footprint, in contrast, means that solar panels contribute in their life cycle to the CO_2 air emissions reduction in comparison with the thermal energy generated by solar panels by burning fossil fuels. Another advantage of solar panels is that at the end of their lifetime, the materials used in solar panels may be almost fully recycled and reused. A negative impact on the environment, however, is associated primarily with the production of aluminium used in solar panels. The aluminium production process requires huge amounts of water which, to a large extent, is disposed of as wastewater or red mud in alumina production. Moreover, the aluminium production process requires high consumption of electricity that is still largely generated in Slovenia by burning fossil fuels. The heat that is released in the aluminium production processes is almost entirely discharged into the environment.

Other heating systems operating in accordance with the solar radiation exploitation principle have characteristics and properties similar to solar panels. Energy payback time ranges from

less than a year to three years. Carbon footprints of solar heating systems are negative, which means that they generate far fewer greenhouse gases than by using fossil fuel heating appliances. For example, a photovoltaic panel reduces greenhouse gas emissions, namely by 0.6 kg CO_2 for each kWh of energy produced. Furthermore, energy for the manufacture of photovoltaic panels is 30 times lower than the energy generated by a photovoltaic panel in its lifetime. The advantage of solar panels in comparison with other solar panels lies mainly in the fact that the materials used for the manufacture of solar panels can be easily almost fully recycled and reused.

References

[1] **Z. Chen, S. Furbo, B. Perers, J. Fan, E. Andersen:** Efficiencies of flat plate solar collectors at different flow rates, Energy Procedia, Vol. 30, p.p. 65 – 72, 2012

[2] **J. Avsec, U. Novosel:** Application of alternative technologies in combination with nuclear energy, Transactions of FAMENA, ISSN 1333-1124, vol. 40, spec. issue 1, p.p. 23-32, 2016

[3] The European Commission's science and knowledge service, Available: http://re.jrc.ec.europa.eu/pvgis/apps4/pvest.php (10.07.2020)

[4] ISO 14040. Environmental management – Life cycle assessment – Principles and Framework.

[5] ISO 14025. 2006. Environmental labels and declarations – Type III environmental declarations – Principles and procedures.

[6] **I. Millera, E. Gençera, S. H. Vogelbauma, R. P. Browna, S. Torkamanid, M. F. O'Sullivana**: Parametric modeling of life cycle greenhouse gas emissions from photovoltaic power, Applied Energy, Vol. 238, p.p. 760–774, 2019

[7] **B. Kim, C. Azzaro-Pantel, M. Pietrzak-David, P. Maussion:** Life cycle assessment for a solar energy system based on reuse components for developing countries, Journal of Cleaner Production, Vol. 208, p.p. 1459-1468, 2019

[8] Talum, d. d., Tovarniška cesta 10, SI-2325 Kidričevo, Slovenija, Available: http://www.talum.si/ (10.07.2020)

[9] Ecoinvent Database, Available: https://www.ecoinvent.org/database/database.html, (10.07.2020)

[10] Eurostat, https://ec.europa.eu/eurostat, Available: (10.07.2020)

[11] **D. J. Gielen, A. W. N. Van Dril:** The basic material industry and its energy use, Prospects for the Dutch energy intensive industry, ECN-C-97-019

[12] **S. H. Farjana, N. Huda N, M. A. Mahmud:** Impacts of aluminum production: A cradle to gate investigation using life-cycle assessment, Science of the Total Environment, Vol. 663, p.p. 958–970, 2019

[13] U.S. Energy Requirements for Aluminum Production, Industrial Technologies. Program Energy Efficiency and Renewable Energy U.S. Department of Energy, 2007

[14] Calculation of fuel consumption per mile for various ship types and ice conditions in past, present and in future, Arctic Climate Change, Economy and Society, 2014)

[15] ARSO, http://www.arso.gov.si/vreme/napovedi%20in%20podatki/vreme_avt.html, Available: (10.07.2020)

Journal of Energy Technology

JET Volume 13 (2020) p.p. 27-36
Issue 2, September 2020
Type of article 1.01
www.fe.um.si/en/jet.html

A REVIEW OF THE USE OF RANKINE CYCLE SYSTEMS FOR HYDROGEN PRODUCTION

PREGLED SISTEMOV Z RANKINOVIM PROCESOM ZA PROIZVODNJO VODIKA

Urška Novosel[1✉], Jurij Avsec[1]

Keywords: Rankine cycle, hydrogen production, electrolysis, thermochemical process

Abstract

The vast majority of steam power plants in the world are based on the Rankine cycle. It is a well-known, trustworthy process that uses water or water vapour as a working medium, which supplies heat from various primary energy sources: fossil fuels, renewable energy sources (solar energy, energy from wood biomass, etc.) or a combination of both. With the Rankine cycle, energy sources other than electricity can be produced, which can be used as the primary energy source for various applications. The present article focuses on the production of hydrogen in addition to electricity; therefore, two energy sources are obtained from the same system with a few modifications of the existing power plant for further exploitation. There are several processes for hydrogen production using the Rankine cycle; in the present article, two processes are focused on: using part of the electricity produced and obtaining hydrogen by electrolysis of water or using part of high quality steam (basically heat energy) in combination with electricity and obtaining hydrogen by a thermochemical copper-chlorine process. Each of these processes has its advantages and disadvantages, which are presented in the present article with an example model of a power plant.

Povzetek

Velika večina elektrarn na svetu, ki uporabljajo parni proces za proizvodnjo električne energije, temelji na Rankinovem procesu. Gre za dobro znan zanesljiv proces, ki kot delovni medij največkrat uporablja

✉ Corresponding author: Urška Novosel, University of Maribor, Faculty of Energy Technology, Hočevarjev trg 1, SI-8270 Krško, Slovenia, Tel.: +386 7 6202 213, E-mail address: urska.novosel@um.si

[1] University of Maribor, Faculty of Energy Technology, Hočevarjev trg 1, SI-8270 Krško, Slovenia

vodo oz. vodno paro, kateri lahko dovajamo toploto iz različnih primarnih virov energije – fosilna goriva, obnovljivi viri energije (sončna energija, energija iz lesne biomase ipd.) ali pa kombinacija obojih. S pomočjo Rankinovega procesa lahko proizvajamo tudi druge vire energije, razen električne energije, ki jih nato uporabimo kot primarni vir energije za različne aplikacije. Članek se fokusira na proizvodnjo vodika poleg električne energije, kar pomeni, da iz istega sistema pridobimo dva vira energije za nadaljnje izkoriščanje, s čimer z nekaj modifikacijami izkoristimo obstoječe elektroenergetsko postrojenje za več namenov. Obstaja več procesov za pridobivanje vodika s pomočjo Rankinovega procesa, toda v članku se bomo osredotočili na dva procesa, in sicer lahko uporabimo del proizvedene električne energije in vodik pridobivamo z elektrolizo vode, lahko pa uporabimo tudi del visokokakovostne pare (v bistvu toplotno energijo) v kombinaciji z električno energijo in vodik pridobivamo s termokemičnim baker-klorovim procesom. Vsak od omenjenih procesov ima svoje prednosti in slabosti, ki bodo predstavljene v članku na konkretnem primeru modela elektrarne.

1 INTRODUCTION

According to various forecasts, energy demand will strongly increase in the coming decades, so it makes sense to make the best of existing systems, especially through the optimization and production of clean energy sources. Hydrogen is certainly a clean source of energy (besides electricity) and highly applicable in several sectors, mainly in industry and transport.

Throughout the world, about 80% of electricity is generated from fossil fuels and nuclear energy, *[1]*. These power plants mostly use the Rankine cycle as a process to convert primary energy source to electricity and possibly heat. The aforementioned products of the Rankine cycle can be used to produce hydrogen by electrolysis (using solely by electricity) or by a thermochemical copper-chlorine (Cu-Cl) cycle (using heat and electricity). However, an even greater change for the better would be if the Rankine cycle used renewable energy sources as a primary energy source.

The present article deals with a model of a conventional steam power plant, in which part of the generated electricity and heat is used to produce hydrogen. The article contains an example of thermodynamic calculation and a comparison of two different cases.

2 RANKINE CYCLE AND HYDROGEN PRODUCTION

The process model is a Rankine cycle power plant, in which two different processes were taken into consideration. First, we remodelled a steam power plant to a cogeneration plant (adding process heater in the cycle), since the heat is required for the Cu-Cl cycle to produce hydrogen, *[2],* (see Fig. 1). For the second case, we made no changes in the Rankine cycle, since only electricity is required for the hydrogen production by electrolysis, *[3],* (see Fig. 2). In both cases, the operating conditions are steady, and the process operates throughout the year (8,760 hours).

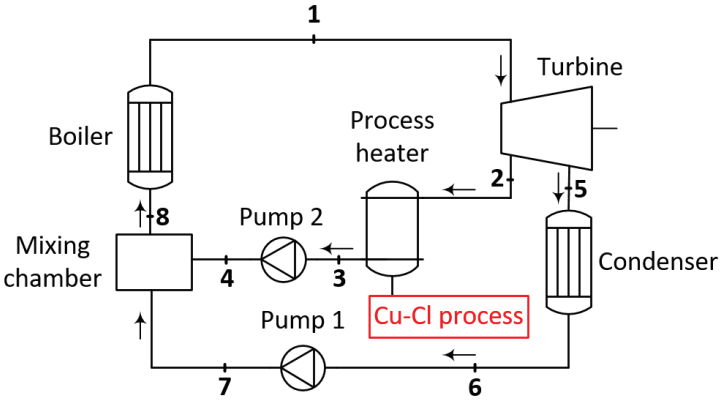

Figure 1: *Rankine cycle producing hydrogen by Cu-Cl process*

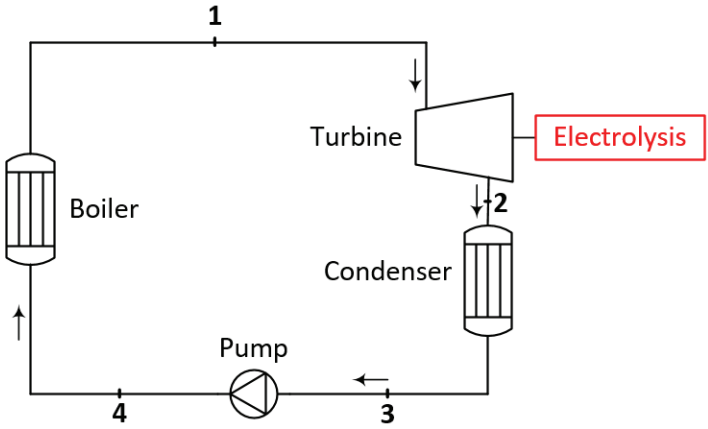

Figure 2: *Rankine cycle producing hydrogen by electrolysis*

Input data for the steam before entering the turbine are 8 MPa and 600 °C, and the mass flow rate is 50 kg/s. Pressure drops and heat losses are disregarded. Steam leaves the process heater and the condenser as a saturated liquid. The isentropic efficiency of the turbine is 80%; the pumps are isentropic.

In the first case, when producing hydrogen by the Cu-Cl process, 30% of the steam is extracted from the turbine at 5.5 MPa for process heating. As in *[2],* the maximum temperature required for the Cu-Cl cycle is 530 °C (see Fig. 3); therefore, the steam cannot expand to pressure lower than 5.5 MPa (temperature of the steam in state 2 (see Fig. 1) is 543 °C) before entering the process heater. Another 70% of the steam continues to expand to 5 kPa in the condenser.

In the second case, when producing hydrogen by electrolysis, the entire mass flow of the steam is expanded in the turbine from 80 MPa to 5 kPa in the condenser.

2.1 Thermochemical Cu-Cl cycle

In the copper-chlorine cycle, water is split into hydrogen and oxygen through intermediate Cu-Cl compounds. The maximum temperature in the cycle is 530 °C. The schematic of a Cu-Cl cycle is in Fig. 3, *[4]*. The chemical reactions of the four steps in the Cu-Cl cycle with the temperature range are, *[5]*:

$2CuCl_{(aq)} + 2HCl_{(aq)} \rightarrow H_{2(g)} + 2CuCl_{2(aq)}$ 90 °C

$CuCl_{2(aq)} \rightarrow CuCl_{2(s)}$ 150 °C

$2CuCl_{2(s)} + H_2O_{(g)} \rightarrow CuO{\cdot}CuCl_{2(s)} + 2HCl_{(g)}$ 400 °C

$CuO{\cdot}CuCl_{2(s)} \rightarrow 2CuCl_{(l)} + ½O_{2(g)}$ 500 °C

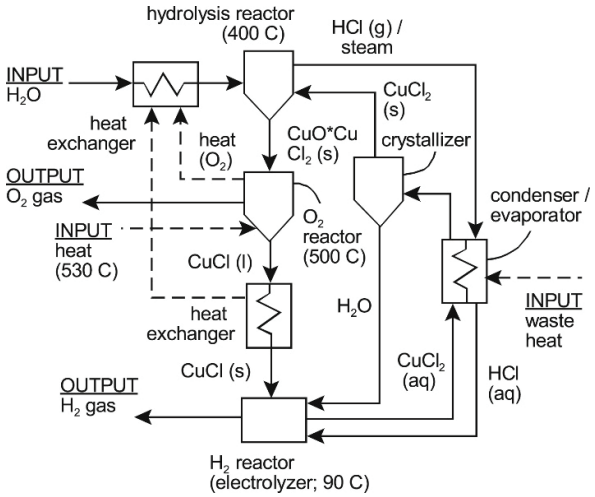

Figure 3: *Schematic of a Cu-Cl cycle*

The Cu-Cl cycle requires heat and electricity for hydrogen production. It has higher conversion efficiency than electrolysis and many other advantages over other methods for hydrogen production, including lower maximum temperature than other thermochemical cycles, *[2]*. Energy requirements for the process, used as input data for the calculation, are shown in Fig. 4, *[6]*.

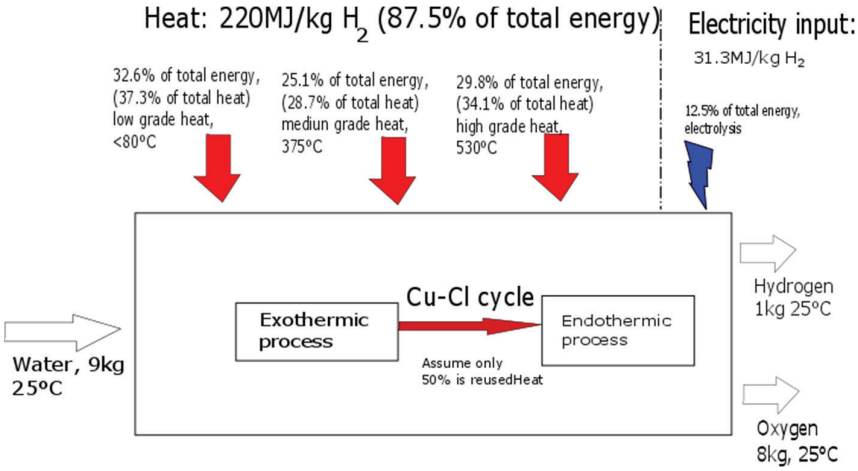

Figure 4: *Energy requirements for the Cu-Cl cycle*

We also took into consideration the amount of energy required to compress hydrogen; thus, the overall energy requirements for the production of 1 kg of hydrogen by Cu-Cl cycle are 220 MJ of heat and 31.3 MJ of electricity and for the compression 15 kWh of electricity, *[6]*.

2.2 Electrolysis

Electrolysis is a chemical process by means of which the reduction and oxidation of chemical compounds are made using a direct electric current to drive a chemical reaction. The electrolysis of water (also called water splitting) is a process by which water is decomposed into hydrogen and oxygen using a minimum electrical voltage of 1.229 V, *[3]*. The chemical reaction is:

$$2H_2O_{(l)} \rightarrow 2H_{2(g)} + O_{2(g)}$$

In thermodynamic terms, the total enthalpy required to decompose water into hydrogen and oxygen is given by Eq. (2.1):

$$\Delta H = \Delta G + T\Delta S \tag{2.1}$$

In Eq. (2.1), ΔH is the reaction enthalpy, under standard conditions it is ΔH_f^0=-285.83 kJ/mol, ΔG is the difference in Gibbs free energy (required electricity) and $T\Delta S$ is the amount of heat absorbed from the environment, *[3]*.

Also, in this case, we took into consideration the amount of energy required to compress hydrogen; thus, the overall energy requirements for the production of 1 kg of hydrogen by electrolysis are 55 kWh of electricity for hydrogen production and 15 kWh of electricity for its compression.

3 THERMODYNAMIC ANALYSIS

We made calculations for each of the cases mentioned above at the specified conditions. The process in Fig. 1 is also drawn in the T-s diagram and is shown in Fig. 5. In Table 1, all input data, pressures, and enthalpies at various steam states are collected for the case. When producing hydrogen by the Cu-Cl process, the rates of process heat supply and heat input, as well as the power produced, are given by Eq. (2.2), (2.3) and (2.4), *[7]*:

$$\dot{Q}_{PH} = 0.3\dot{m}_1(h_2\text{-}h_3) \tag{2.2}$$

$$\dot{Q}_{in} = \dot{m}_1(h_1\text{-}h_8) \tag{2.3}$$

$$\dot{W}_t = 0.3\dot{m}_1(h_1\text{-}h_2) + 0.7\dot{m}_1(h_2 - h_5) \tag{2.4}$$

Steam enters the turbine at state 1, 30% of steam is extracted from the turbine at state 2 for process heating; another 70% of steam expands further to state 5. Steam enters the condenser, where it is condensed at a constant pressure to state 6 and then pumped to state 7. After the process heater, the steam is saturated liquid (state 3) and then pumped to state 4. Both steam fractions enter the mixing chamber and leave it at state 8 (see Fig. 1 and 5).

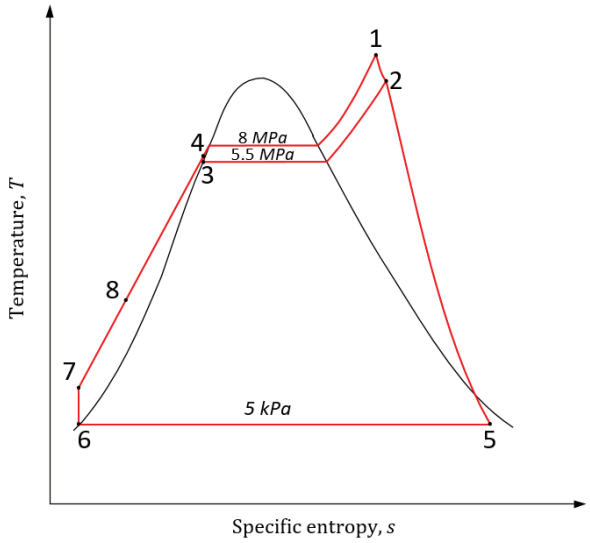

Figure 5: *T-s diagram Rankine cycle with process heater*

Table 1: *Input data, pressures and enthalpies for Rankine cycle with Cu-Cl process*

Steam state	Mass flow rate [kg/s]	Pressure [MPa]	Enthalpy [kJ/kg]
1	50	8	3642.38
2	15	5.5	3530.69
3	15	5.5	1185.09
4	15	8	1188.35
5	35	0.005	2427.33
6	35	0.005	137.75
7	35	8	145.79
8	50	8	458.56

In the second case, we have a basic Rankine cycle process without a process heater (see Fig. 2). The process is also drawn in the T-s diagram and is shown in Fig. 6. In Table 2, all input data, pressures, and enthalpies at various steam states are collected for that case. When producing hydrogen by electrolysis, the rate of heat input and the power produced are expressed in Eq. (2.5) and (2.6), *[7]*:

$$\dot{Q}_{in} = m(h_1 - h_4) \tag{2.5}$$

$$\dot{W}_t = m(h_1 - h_2) \tag{2.6}$$

Steam enters the turbine at state 1, and leaves it at state 2, then enters the condenser where it is condensed at a constant pressure to state 3 (saturated liquid) and pumped to state 4.

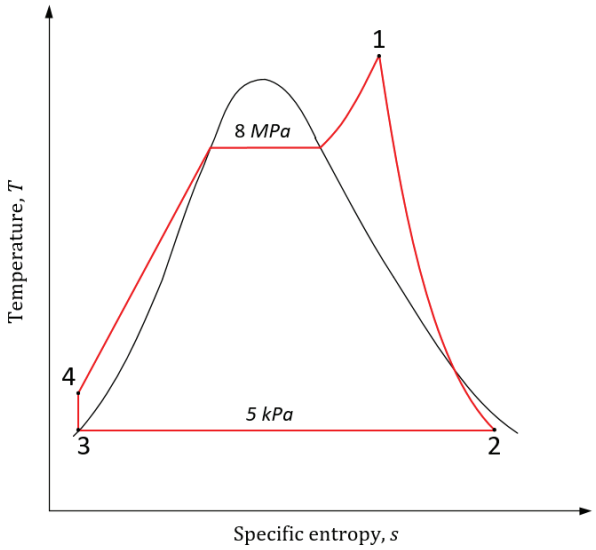

Figure 6: *T-s diagram Rankine cycle*

Table 2: *Input data, pressures and enthalpies for Rankine cycle with electrolysis*

Steam state	Mass flow rate [kg/s]	Pressure [MPa]	Enthalpy [kJ/kg]
1	50	8	3642.38
2	50	0.005	2441.24
3	50	0.005	137.75
4	50	8	145.79

For both cases, we calculated efficiencies. The Rankine cycle with a process heater is basically a cogeneration plant; the efficiency for this process is also called the "utilization factor", *[7],* and can be calculated by means of Eq. (2.7); the thermodynamic efficiency for the second case is written in Eq. (2.8). The power of the pumps is almost negligible, so this was not taken into consideration.

$$\epsilon_u = \frac{\dot{W}_t + \dot{Q}_{PH}}{\dot{Q}_{in}} \tag{2.7}$$

$$\eta_{TD} = \frac{\dot{W}_t}{\dot{Q}_{in}} \tag{2.8}$$

4 RESULTS AND DISCUSSION

When producing hydrogen by the Cu-Cl process, heat and electricity are required, so the Rankine cycle is used not only for electricity production but also for heat (process heating unit), resulting in lower turbine power output. With this cogeneration plant, the rate of process heat is 35.18 MW, and turbine power output is 44.2 MW. The rate of heat input in the boiler is 159.19 MW. Thus, the utilization factor, which was calculated with Eq. (2.7), is 50%.

The rate of process heat is the input data to calculate the amount of hydrogen produced by the Cu-Cl process. The system operates 8,760 hours per year, so the available heat is 308,177 MWh. This heat energy is enough to produce 5,043 tons of hydrogen per year or 13.82 tons of hydrogen per day. Then how much electricity is available per year and how much electricity is needed to produce 13.82 tons of hydrogen per day were calculated. Per year, 387,192 MWh of electricity is available; the amount of electricity required for the production and compression of 13.82 tons of hydrogen is 119,489 MWh, which means we use about 30.9% of generated electricity.

In a second case, producing hydrogen by electrolysis solely with electricity is required. With the basic Rankine cycle power plant, the turbine power output is 60.1 MW. The rate of heat input in the boiler is 174.83 MW. Thus the thermodynamic efficiency, which was calculated with Eq. (2.8), is 34.4%.

For an extreme case, which is impossible in practice, when all of the electricity generated in the Rankine cycle power plant is used for the hydrogen production and compression, the amount of produced hydrogen has been calculated. Per year 526,476 MWh of electricity is available, which is enough to produce 7,521 tons of hydrogen per year or 20.6 tons of hydrogen per day. If the same percentage of electricity as in the previous case (30.9% of generated electricity) is used, the

amount of produced hydrogen would be 2,324 tons of hydrogen per year or 6.37 tons of hydrogen per day.

Thermodynamic results for both cases are shown in Table 3.

Table 3: *Calculation results*

	RC + Cu-Cl process	**RC + electrolysis**
$\dot{Q}_{PH}$ [MW]	35.18	/
$\dot{Q}_{in}$ [MW]	159.19	174.83
$\dot{W}_t$ [MW]	44.2	60.1
ϵ_u/η_{TD}	0.50	0.344
H_2 produced [t/day]	**13.82**	100 % of electricity **20.6**
		30.9 % of electricity **6.37**

The calculation results show that a higher amount of hydrogen is produced by the Rankine cycle with a process heater for the Cu-Cl process; since the use of 100% of generated electricity is not realistic, the power supply must always be provided, but there may be a surplus of generated electricity, which can be used for other purposes, such as hydrogen production. If only 30.9% of electricity generated is used, more than half as much hydrogen as in the first case can be produced. Perhaps it makes sense to use also heat, not only electricity but also for hydrogen production, since the electricity is more widely used for many other applications and is easily convertible into other forms of energy.

5 CONCLUSION

The present article shows that it makes more sense to produce hydrogen by Cu-Cl process when a Rankine cycle power plant is the source of heat and electricity to drive a hydrogen production process. The article also gives many cues for future work, such as increased efficiency with modifications of the Rankine cycle; adding reheating or regeneration. It would be interesting to make an exergy and economic analysis and then compare results. However, more accurate results would be obtained by building a dynamic model for the chosen hydrogen production process.

References

[1] **International Energy Agency:** *Electricity generation by source.* Available: https://www.iea.org/data-and-statistics (15. 6. 2020)

[2] **Z. L. Wang, G. F. Naterer**: *Greenhouse gas reduction in oil sands upgrading and extraction operations with thermochemical hydrogen production,* International Journal of Hydrogen Energy, Vol. 35, Iss. 21, p.p. 11816 – 11828, 2010

[3] **D. A. J. Rand, R. M. Dell:** *Hydrogen Energy,* RSC Publishing, 2008

[4] **G. F. Naterer, S. Suppiah, L. Stolberg, M. Lewis, Z. Wang, M. A. Rosen, I. Dincer, K. Gabriel, A. Odukoya, E. Secnik, E. B. Easton, V. Papangelakis:** *Progress in thermochemical hydrogen production with the copper-chlorine cycle,* International Journal of Hydrogen Energy, Vol. 40, Iss. 19, p.p. 6283-6295, 2015

[5] **G. Naterer, S. Suppiah, M. Lewis, K. Gabriel, I. Dincer, M. A. Rosen, M. Fowler, G. Rizvi, E. B. Easton, B. M. Ikeda, M. H. Kaye, L. Lu, I. Pioro, P. Spekkens, P. Tremaine, J. Mostaghimi, J. Avsec, J. Jiang:** *Recent Canadian advances in nuclear-based hydrogen production and the thermochemical Cu-Cl cycle,* International Journal of Hydrogen Energy, Vol. 34, Iss. 7, p.p. 2901-2917, 2009

[6] **J. Avsec, U. Novosel, Z. Wang:** *Thermoeconomic analysis of combined solar thermal power plant with hydrogen production process.* Proceedings of ICCE 2016. Ottawa: International Academy of Energy, Minerals and Materials, p.p. 63-73, 2016

[7] **Y. A. Çengel, M. A. Boles:** *Thermodynamics: An Engineering Approach, Eighth edition,* McGraw-Hill Education, 2015.

Nomenclature

(Symbols)	(Symbol meaning)
h, H	enthalpy
G	Gibbs free energy
T	temperature
s, S	entropy
$\dot{Q}$	heat rate
$\dot{m}$	mass flow rate
$\dot{W}$	power
ϵ	utilization factor
η	efficiency

Journal of Energy Technology

JET Volume 13 (2020) p.p. 37-44
Issue 2, September 2020
Type of article 1.01
www.fe.um.si/en/jet.html

REVERSIBLE PUMP-TURBINES – A STUDY OF PUMPING MODE OFF-DESIGN CONDITIONS

REVERZIBILNE TURBINE-ČRPALKE – ANALIZA NESTACIONARNIH POJAVOV V ČRPALNEM REŽIMU OBRATOVANJA

Uroš Ješe[✉], Aleš Skotak[1]

Keywords: Pump-Turbine, Rotating stall, Cavitation, Pumping mode instabilities

Abstract

The role of pumped storage power plants (PSP) in electrical grid systems has been changing in recent years. Demands for switching from pumping to generating mode are becoming increasingly frequent. Moreover, the operating ranges of the reversible pump-turbines used in PSP systems are becoming wider in order to use the PSP as a regulator and a stabilizer of the electrical grid. The primary challenges in the development of pump-turbines are the hydraulic instabilities that occur in pumping and generating modes. The present paper focuses on partial load pumping mode instabilities, such as cavitation and rotating stall. Modern tools, such as CFD, are used for the analysis of the phenomena along with conventional experimental approaches. Rotating stall has been investigated in hydraulic laboratory experimentally and reproduced numerically using commercial CFD code. Three rotating stall cells with a rotational frequency of 2.5% of nominal pump-turbine frequency have been identified. Cavitating vortices related to rotating stall were found in the guide vanes region. Both phenomena indicate highly unstable and potentially dangerous operating conditions that need to be investigated in detail. Understanding the causes for the instabilities will lead to an improved pump-turbine design that will enable safer, more flexible and more reliable operating with fewer unwanted instabilities.

[✉] Corresponding author: Uroš Ješe, PhD, Litostroj Power d.o.o., Litostrojska 50, 1000 Ljubljana, Slovenia, uros.jese@litostrojpower.eu

[1] Aleš Skotak, PhD, Full time: Litostroj Engineering a.s., Čapkova 2357/5, 678 01 Blansko, Czech Republic, ales.skotak@litostrojpower.com

Povzetek

Vloga črpalnih hidroelektrarn v električnih omrežjih se v zadnjih letih spreminja. Zahteve po prehodu s črpalnega v turbinski režim in nazaj postajajo vse pogostejše. Območja obratovanja reverzibilnih črpalk-turbin se ob tem širijo, saj se črpalne hidroelektrarne uporabljajo kot regulator in stabilizator električnega omrežja. Glavni izzivi pri razvoju reverzibilnih črpalk-turbin so hidravlične nestabilnosti, ki se pojavijo v črpalnem in turbinskem režimu. Članek se osredotoča na nestabilnosti v črpanem režimu pri delnih obremenitvah, kot sta kavitacija in vrteče zastojne celice. Sodobna orodja, kot računska dinamika tekočin (CFD), se uporabljajo za analizo pojavov kot dodatek klasičnim eksperimentalnim pristopom. Vrteče zastojne celice so bile eksperimentalno raziskane v hidravličnem laboratoriju ter numerično reproducirane s komercialnim CFD programom. Odkrite so bile tri zastojne celice s frekvenco vrtenja 2.5 % nazivne frekvence črpalke-turbine. V območju vodilnih lopat so bili opaženi kavitacijski vrtinci povezani z zastojnimi celicami. Oba pojava kažeta na zelo nestabilno in potencialno nevarno obratovanje, ki ga je potrebno podrobno raziskati. Razumevanje vzrokov za nestabilnosti bo pripeljalo do izboljšane zasnove črpalke-turbine, ki bo omogočila varnejše, prožnejše in zanesljivejše obratovanje z manj neželenimi nestabilnostmi.

1 INTRODUCTION

The market for pumped storage power plants (PSP) is growing every year. The main reason is the increasing number of weather-conditioned sources of energy, such as wind and solar power plants. To provide a reliable electrical grid, power plants that can balance the differences between demand and supply of electricity must be included. A PSP with reversible Francis runner that has a wide operating range and enables a fast transition from the generating to the pumping mode is highly suitable for this task. Besides new PSP projects, refurbishments of the pump-turbine runners represent an important part of the market.

The development process of a new pump-turbine runner is related to several major challenges. The customer demands and final goals of the development process are the operation of the pump-turbine from zero to maximum output in the generating mode and non-restricted operation in the pumping mode. To achieve that, the whole operating range should be free of hydraulic instabilities. An additional reason for the refurbishment is frequently the improvement of the total efficiency of the cycle. The development of the new runner with the expected reliability and performance must be supported by effective cooperation among hydraulic and mechanical designers and by the application of precise manufacturing technology.

Both generating and pumping mode instabilities have been analysed during this study in order to prepare the new runner design for a 2×325 MW pump storage powerplant in Dlouhe Strane in the Czech Republic, which will be able to operate from 0–100% output power, *[1].*

The main instability in the generating mode is considered the S-shaped curve close to the runaway operating point. It has been studied numerically and experimentally by various researchers, *[2, 3, 4, 5, 6].* In contrast, cavitation and rotating stall are considered to be the main hydraulic instabilities in the pumping mode operation. Cavitation in the pumping mode regime mostly occurs at the impeller leading edge, where local pressure drops to vaporization pressure. However, in combination with the phenomenon called rotating stall, it is possible that the cavitation also occurs in the high-pressure distributor region.

Rotating stall is a phenomenon present at partial load operation and was first investigated for the compressor applications, *[7].* In recent years, the problem became highly relevant in the field of pump-turbines, which lead to several studies, [8, 9, 10]. The rotating stall is sometimes related to the positive slope of the performance curve also called hump zone, *[11]*, which is an unstable and potentially dangerous operating region. Fig. 1 shows typical pump-turbine characteristics for pumping regime in a non-dimensional form (Φ – flow rate coefficient, Ψ – specific energy coefficient, ω – rotational speed, ω_s – rotating stall rotational speed). If present, it can lead to uncontrollable changing of the discharge through the machine and consequently strong vibrations. The intensity of the rotating stall in pump-turbines can vary. As shown several times, experimentally and numerically, *[8, 11, 12]*, changing discharge and guide vane opening angle can lead into a different number of the stalled cells and a different rotating stall frequency. Various shapes of rotating stall influence pressure fluctuations, radial forces acting on the impeller as well as guide vanes vibrations related to the torque fluctuations. If the rotating stall is very intense, the appearance of the cavitating vortex is possible in the distributor region. Operating under the described conditions should be completely avoided. However, rotating stall can be present even if the slope on the performance curve is negative.

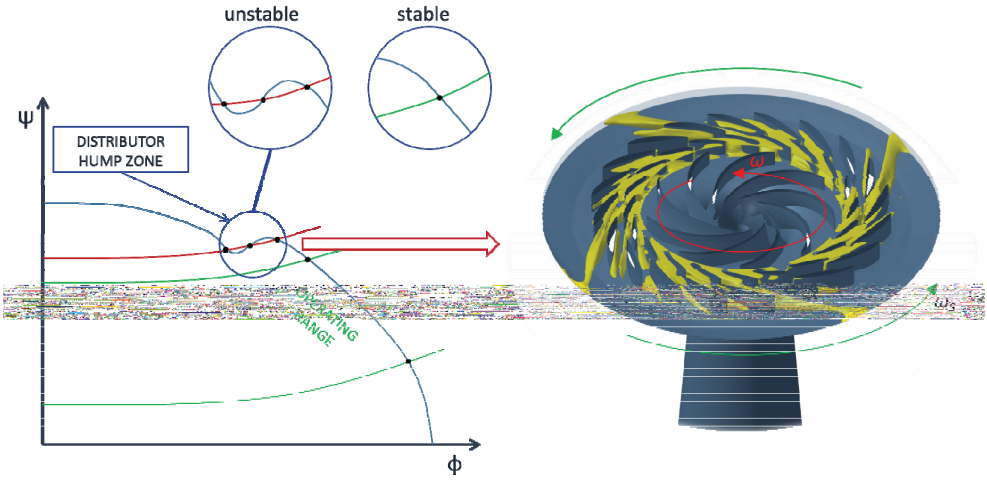

Figure 1: *Pumping mode operating range with distributor hump and related rotating stall*

Rotating stall has been investigated experimentally and numerically in order to propose a hydraulic design that would be free of instabilities and would satisfy very demanding criteria of non-restricting operation.

2 EXPERIMENT

Experimental measurements took place in Litostroj Engineering hydraulic laboratory, *[12].* Additional to the standard performance measurement, eight (8) pressure sensors have been distributed around vaneless space between the impeller and the guide vanes. The rotational speed of the model pump-turbine has been set to n = 1400 min^{-1}. Even though the whole range of guide vane openings has been measured, one constant guide vane opening a_0 = 20 mm is presented and analysed in the paper. The guide vane channel and vaneless space have been

observed during the measurements by installing Plexiglas window in the distributor region. The goal of the experimental setup was to measure low-frequency pressure pulsations in pumping and generating mode. Measurements have been done for the entire part load regime, however, for the analysis, operating points at the best efficiency point (BEP) $Q = Q_{BEP}$ and at $Q = 0.65\ Q_{BEP}$ have been chosen and will be presented.

Fig. 2 shows pressure fields around the distributor at $Q = 0.65\ Q_{BEP}$. Three pressure cells are formed and are rotating around the distributor with governing frequency $f = 0.59$ Hz, which corresponds to around 2.5 % of the pump-turbine rotation frequency. The relationship between pressure fields and velocity contours obtained by CFD and presented on Fig. 4 have been discussed in detail by *[10]* together with governing mechanisms of rotating stall on different pump-turbine geometry and indicate the presence of the rotating stall. In contrast, the flow has been stable with no pressure pulsations at the $Q = Q_{BEP}$. The level of low-frequency pressure oscillations has been presented in *[13]* and reached ±15 % of the average pressure level around the distributor.

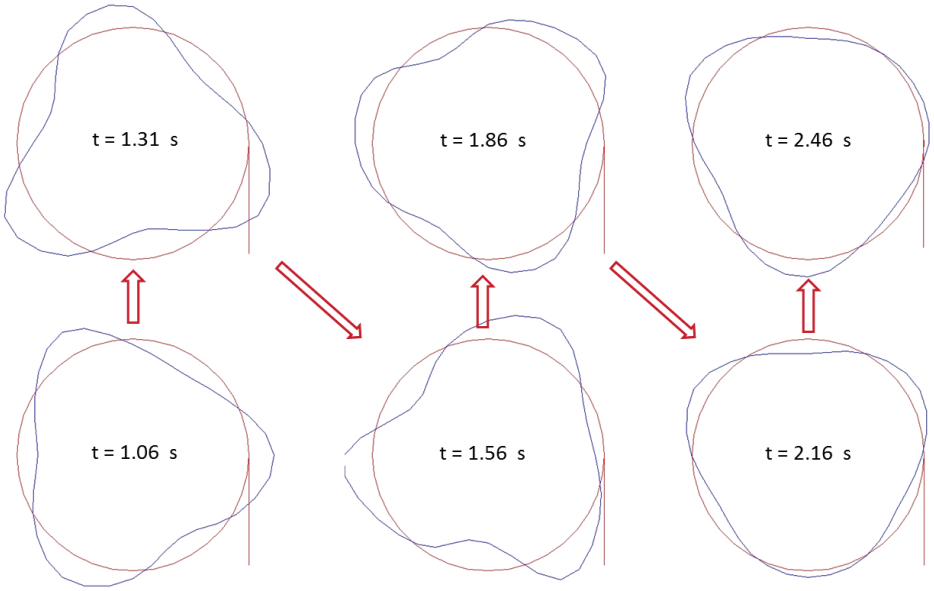

Figure 2: *Pressure fields around the distributor at $Q = 0.65Q_{BEP}$ at different time steps*

Occasionally, during the pressure measurements at $Q = 0.65\ Q_{BEP}$, cavitating vortexes have been observed in the distributor between the guide vanes, as seen in Fig. 3. Sometimes, there was one vortex, attached to the suction side of the guide vane (Fig 3, left). At some other instances, the phenomenon has been observed as several separated, smaller cavitating vortices, as seen in Fig. 3, right. In both cases, the vortices occur only for a short time. It should be pointed out that the cavitation in the distributor region is highly unusual due to very high pressure in the surrounding.

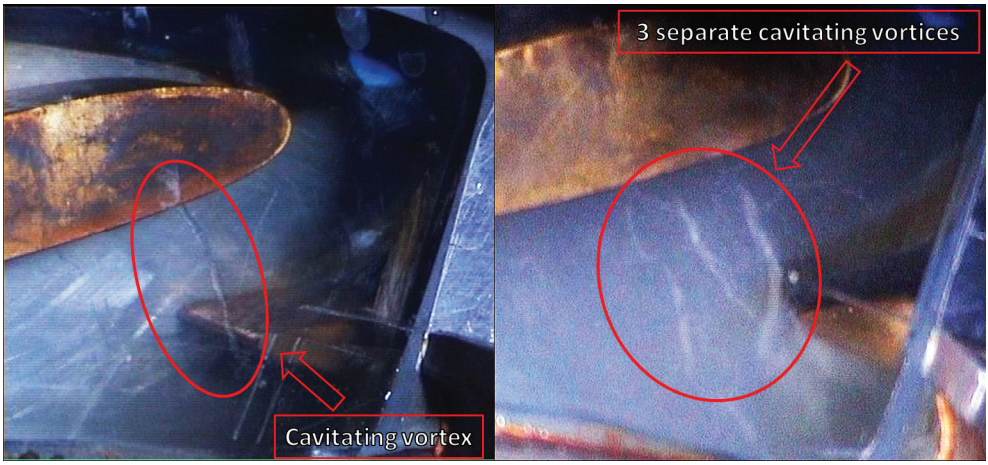

Figure 3: *Cavitating vortices in the distributor region*

3 NUMERICAL ANALYSIS

For the flow analysis, numerical flow simulation (Computational Fluid Dynamics) software is nowadays the most common tool. It uses a set of Navier-Stokes equations to compute the transport of mass and momentum in all parts of the computational domain. Commercial software has been used for the simulation. Transient simulations were performed in the premises of Litostroj Engineering a.s. by using URANS equations and turbulence model based on the k-ε model. Choosing the appropriate turbulence model is essential for the successful reproduction of complex phenomena, such as rotating stall. It should be a robust model to enable convergence with wall functions that enable exact prediction of first flow separation on the guide vanes. The time step corresponds to 2° of the impeller revolution, which has been proved by *[8]* and *[10]* to be a good compromise between quality of results and computational cost. Around 20 revolutions of the impeller have been simulated. Boundary conditions are very important for the stability of the simulations.

Moreover, in some cases, they also have a significant influence on the obtained results, especially at non-optimal flow conditions, such as part load. In our case, constant mass flow rate Q has always been set at the inlet of the domain and at the outlet of the domain, static pressure p_s has been imposed. A no-slip condition has been applied on the solid walls.

The meshing of the domains has been done using commercial software, using structured and unstructured mesh. The total mesh contains around 10 million cells; special attention has been put into meshing the distributor region, since this would be the place where the rotating stall occurs. Dimensionless criteria $y+$ that indicates mesh quality close to the walls has reached mean values around $y+ = 10$ in all parts of the domain.

Unsteady CFD analysis has been focused on the rotating stall parameters and related phenomena. Operating points at $Q = 0.65\ Q_{BEP}$ have been chosen for the comparison to the experiment. Three regions with high velocity have been found (Fig. 4 - right) in between three cells of blocked discharge, which corresponds to the experimental findings. Separation zone regions periodically appeared and disappeared at the guide vanes surfaces (Fig. 4 - left) and

caused backflow from stay vanes and even spiral case region. A detailed description of the complex rotating stall origins is given in *[11].* Numerical rotating stall frequencies have been estimated to 0.5 Hz. Since the frequencies of the rotating stall are very low, more impeller revolutions should be simulated for more accurate frequency prediction. However, we can say that the phenomenon has been accurately described by using CFD and simple k-ε based

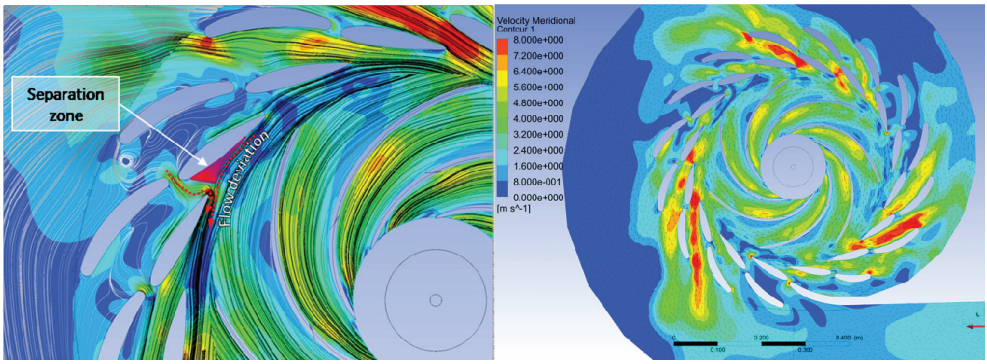

turbulence model.

Figure 4: *Left - Separation zone during rotating stall occurrence; Right - Meridional velocity contour during rotating stall*

Cavitating vortices in the distributor channel have been occasionally observed under rotating stall. The vortex is attached to the guide vanes and reaches the next upstream channel, as seen on Fig. 5. Constant *Q*-criterion has been used for the vortices representation. The estimated time of the cavitating vortex appearance is around 0.011 s, which corresponds to around one quarter of the impeller revolution. The vortex appears and disappears several times at different positions around the distributor during the impeller revolution. The appearance time is very short, which means that the phenomenon is visually demanding to observe. The vortex appears when the discharge through the guide vane channel is partially blocked (Fig. 5). First, the blockage appears at the hub side and later also at the shroud side. The moment when the flow is still strong at the shroud side and blocked at the hub side is favourable for the occurrence of the cavitating vortex in the guide vane channel. A comparison of the experimental and numerical appearance of the cavitating vortex (Figs. 3 and 5) show very good agreement. More post-processing images of the cavitating vortex can be found in *[13].*

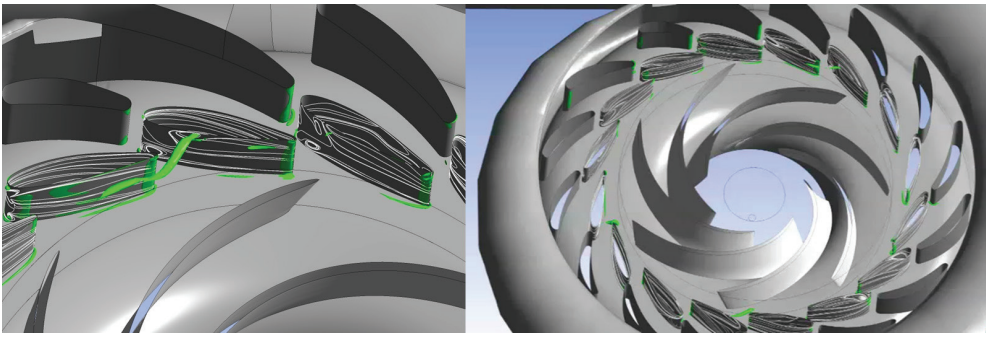

Figure 5: *Numerically simulated cavitating vortex*

4 CONCLUSIONS

The main goal of the study has been to improve the understanding of the instabilities that occur at the off-design operation of the reversible pump-turbine in order to enable a wide operating range at the pumping and generating modes. The present paper has been focused on the partial load pumping mode instabilities, such as rotating stall and cavitation. CFD analysis has been used to successfully reproduce the rotating stall and related cavitating vortex that has been observed during the experiment in the hydraulic laboratory. The numerical governing frequency of the rotating stall is f = 0.5 Hz, and it is a reasonable approximation of experimental value f = 0.59 Hz. A cavitating vortex has been visualized and compared to the experimental one. The analysis explains the governing mechanisms of the cavitating vortex. The methodology can be used for pump-turbine impeller and guide vanes geometry optimization. The ongoing study has been used in the scope of the development project of pump-turbines with reversible Francis runner and non-restricted operating ranges in pumping and generating mode. The first rehabilitation project that includes the findings of the study and enables a wide operating range is Dlouhe Strane PSP in the Czech Republic.

References

[1] **Skotak, A., Stegner, L., Feilhauer, M., Cepa, Z. and Mikulašek, J.** (2017). Designing of pump turbine for restricted range of operation. Proc. HidroVision 2017, USA

[2] **Staubli, T., Widmer, C., Tresch, T. and Sallaberger, M.** (2010). Starting pump-turbines with unstable characteristics. HYDRO 2010

[3] **Nicolet, C., Alligné, S., Kawkabani, B., Simond, J-J. and Avellan, F.** (2009). Unstable operation of Francis pump-turbine at runaway: rigid and elastic water column oscillation modes. Int. J. Fluid Mach. Syst., vol. 2, no. 4, pp. 324–333.

[4] **Frigne, P. and Van den Braembussche, R.** (1984). Distinction between different types of impeller and diffuser rotating stall in a centrifugal compressor with vaneless diffuser. Trans of ASME Journal of Engineering for Gas Turbines and Power 106(2):468-474

[5] **Hasmatuchi, V., Fahrat, M., Roth, S., Botero, F. and Avellan, F.** (2011). Experimental evidence of rotating stall in a pump-turbine at off-design conditions in generating mode. Journal of Fluids Engineering, 133(5):051104

[6] **Jacquet, C., Fortes-Patella, R., Balarac, L. and Houdeline, J-B.** (2016). CFD Investigation of Complex Phenomena in S-Shape Region of Reversible Pump-Turbine. IOP Conf. Ser.: Earth Environ. Sci. 49 042010

[7] **Haupt, U., Seidel, U., Abdel-Hamid, A. and Rautenberg, M.** (1988). Unsteady flow in a centrifugal compressor with different types of vanes diffuser. Trans of ASME Journal of Turbomachinery, 110(3):293-302

[8] **Braun, O.** (2009). Part load flow in radial centrifugal pumps PhD Thesis EPFL, Lausanne

[9] **Pacot, O., Kato, C., Guo, Y., Yamade, Y. and Avellan, F.** (2016). Large eddy simulation of the rotating stall in a pump-turbine operated in pumping mode at a part-load condition Journal of Fluids Engineering, ASME, doi: 10.1115/1.4033423

[10] **Ješe, U.** (2015). Numerical study of pump-turbine instabilities: Pumping mode off-design conditions PhD Thesis, Univ. Grenoble Alpes, Grenoble

[11] **Ješe, U. and Fortes Patella, R.** (2016). Unsteady numerical analysis of the rotating stall in pump-turbine geometry Proc. 28th IAHR symposium on Hydraulic Machinery and Systems, Grenoble

[12] **Veselý, J., Půlpitel, L. and Troubil, P.** (2005). Model research of rotating stall on pump-turbines Proc. HYDRO 2005, Villach

[13] **Ješe, U., et al (2017).** Cavitating vortices in the guide vanes region related to the pump-turbine pumping mode rotating stall J. Phys.: Conf. Ser. 813 012043

Nomenclature

(Symbols)	(Symbol meaning)
a_0	Guide vane opening
f	Frequency
k	turbulent kinetic energy
CFD	Computational fluid dynamics
PSP	Pump storage power plant
Q	Discharge
$y+$	Wall spacing
ε	Dissipation
Φ	Flow rate coefficient
Υ	Specific energy coefficient
ω	Rotational frequency
(Subscripts)	(Subscripts meaning)
s	Stall, static
BEP	best efficiency point
max	maximum

Acknowledgments

Uroš Ješe gratefully acknowledges the support of Slovenian Research Agency (ARRS) conducted through the research project L2-1825.

JET Journal of Energy Technology

JET Volume 13 (2020) p.p. 45-53
Issue 2, September 2020
Type of article 1.04
www.fe.um.si/en/jet.html

THE PROPERTIES OF THE MATERIAL GADOLINIUM AND THE WORKING AGENT USED IN THE INSTALLATION OF MAGNETIC REFRIGERATION DEVICES

LASTNOSTI GADOLINIJA, DELOVNEGA SREDSTVA, KI GA LAHKO UPORABLJAMO V MAGNETNIH HLADILNIH NAPRAVAH

Botoc Dorin[1], Jurij Avsec[2], Adrian Plesca[3] , Gabor Georgel[4] , Rusu Ionut[5]

Keywords: Gadolinium, heat transfer, magneto-calorific, magnetic field

Abstract

Much remains to be done to understand better and thus achieve better control over magnetic materials to maximize their magnetocaloric properties and performance, specifically for gadolinium. A clear path forward is highlighted by thorough experiments coupled with theory, in which the latter is tested and refined against the former, thus resulting in discoveries of new and improved materials and bringing near-room-temperature magnetic refrigeration technology to fruition in the near future.

Povzetek

V prihodnosti bo potrebno še veliko storiti, da bi bolje razumeli magnetne materiale in da bi povečali njihove magnetokalorične lastnosti in zmogljivosti. Še posebej je zanimiv gadolinij. S pomočjo nadaljnjih preizkušanj v povezavi s teorijo bi lahko razvili učinkovite magnetne hladilne naprave na osnovi magnetokaloričnih vplivov magnetnih materialov.

[R] Corresponding author: Botoc Dorin, E-mail address: dorinbotoc@yahoo.com

[1] University of Maribor, Faculty of Energy Technology, Laboratory for Thermomechanics, Applied Thermal Energy Technologies and Nanotechnologies, Hočevarjev trg 1, SI-8270 Krško, Slovenia

[2] Faculty of Electrical Engineering, Energetics and Applied Informatics, Gheorghe Asachi Technical University of Iasi, Department of Power Engineering, Romania

1 INTRODUCTION

A considerable amount of literature has been published in which researchers have highlighted the benefits of using magnetocaloric materials for the refrigeration processes and the efficient energy-saving potential of the magnetic materials. Gao et al. studied in detail the transduction of energy in ferromagnetic and ferroic materials; moreover, the energy transduction in different types of materials such as piezoelectric, electromagnetic, and magnetostrictive materials was discussed in detail, and the relevant advantages and disadvantages were also mentioned, *[1].* In Europe and America, a massive amount of energy is wasted on refrigeration and air conditioning; by adopting an energy-efficient approach, such as magnetocaloric refrigeration or magnetic refrigeration, much of this energy can be saved, *[2].* The main reason for increased interest in magnetic refrigeration is due to its environmental friendly operation, high energy efficiency, and the absence of the need for the usage of harmful gases that cause ozone depletion and other effects that contribute to global warming, *[2].*

2 LITERATURE REVIEW

Efforts are being made for the development of a refrigerator that can work at room temperature. Various successful attempts have been made on the trial or experimental levels, such as the products developed by the companies General Electric and Haier. The properties that contribute to the refrigeration effect are due to the extraordinary response of these materials to external magnetic fields; such properties occur close to the Curie temperature, which is the temperature at which the basic inherent magnetic properties are diminished, and the material temperature is dependent upon the application of the magnetic field, *[3].* The effect has been in use since 1920, for the examination of the magnetic structure and properties of iron and other related elements, *[3].* The magnetocaloric effect was first discovered by the German physicist Warburg in 1881, *[3].* Faraday discovered that the time variation of magnetic flux results in the induction of electric currents, *[3].* Joule's research clarified the important concepts related to the electric currents and associated heat energy and confirmed that heat energy released due to flow of electromagnetically induced current is equivalent to the heat energy produced due to the electric current produced by any other source.

Moreover, it was also inferred that rapid magnetization and demagnetization results in the heating of the magnetic material due to heat energy released as a result of current flow, *[3].* Thomson inferred from the concepts of thermodynamics that the temperature-dependent property of magnetization of any material will represent or exhibit these property-related parameters in the form an increase or decrease in temperature, *[3].* The accurate, quantifiable measurement of the magnetocaloric effect of iron was possible long after the discovery of related phenomena, *[3].*

Issues related to high temperature made the measurement of the related parameters challenging. The heat-based electric motor was presented and produced by Tesla, Edison, and Stefan, *[3].* Weiss and Langevin separately contributed considerable knowledge and understanding about temperature ranges, magnetization, and hysteresis, *[3].* The initiation of studies on low temperature that had ultimately led to the realization and theoretical formulation of refrigeration was independently reported by Debye and Giauque, who demonstrated that

adiabatically demagnetized paramagnetic salts result in the attainment of low temperatures; Giauque and MacDougall showed the very low-temperature achievements with such salts, *[3].*

All the work reported above resulted in the development of the foundation for the concepts of the building and understanding of magnetism, temperature, and material properties. Pecharsky et al. reported that the magnetic dipole moments of Gd could be aligned at room temperature (294 K), and highlighted that the continuous magnetic refrigeration was experimentally shown by the Collins and Zimmerman, who tested magnetic refrigerators operating at very low-temperature ranges, *[4].*

Zimm and DeGregoria explained the basic mechanism of the active magnetic regenerator cycle, *[4].* Kitanovski et al. highlighted that the there is a need to develop new thermodynamic cycles that can explain the magnetic refrigeration phenomena accurately and comprehensively; they also reported many publications about the Bryton and Ericsson's cycle associativity with the magnetic refrigeration. Moreover, active magnetic regenerators with various thermodynamic cycles were analysed, and numerical simulation of AMR was also performed using the finite element method, *[5]*. The AMR operating on the Brayton cycle resulted in the production of highest cooling power capability, while AMR operating on the Ericsson cycle is the most efficient one, *[5]*; they also mathematically explained the numerical aspects of AMR simulation. Wolf et al. provided a quantum-based explanation of the magnetocaloric effect and proposed an increase in the change in the entropy with respect to change in the magnetic field close to magnetically achieved quantum-critical point by the accurate and precise measurement of calorimetric effect, *[6].*

Noume et al. used COMSOL of simulation of the magnetocaloric effect for the designing of the magnetic regeneration cycle for the electric vehicles, *[7].* As an electric vehicle operates on the battery, in the simulation performed, the fluid flow (mainly laminar), heat transfer in solids and fluids was used, and the velocity, temperature, and heat transfer coefficient were studied *[7].* The primary equation used for the fluid flow is the Navier-Stokes equation; the energy equation, along with the heat transfer equations, were mainly used, *[7].* Gobi and Sahu used COMSOL to perform the exploratory study of the magnetocaloric effect on three different materials; these materials were gadolinium and two other different alloys for the evaluation of the final temperature of the magnetic material; the gadolinium showed the adiabatic temperature difference of 12 K, which was the highest among the studied material, *[8].* An application was developed with a graphical user interface (GUI) so that the user can input different variables, and visualize the contours of temperature and other variables.

The comprehensive literature review has been performed in this study for understanding the main developments in the selected domain. Moreover, the phenomena were also explained in detail to develop a sense of understanding. The research and publication trend in the field of magnetocaloric effect has significantly increased by the end of the 20th century due to the need for energy-efficient refrigeration and air-conditioning systems. The focus of the literature study was to report the relevant findings related to phenomena and an exploration of the numerical formulation aspects of the magnetocaloric effect. The scientific literature available on the topic of magnetocaloric effect can be subdivided into many types for the relevancy and domain specification. These categories are material-oriented, mathematical based, experiment-based, numerical based, and thermodynamic based.

This material-oriented study is focused on the determination of material constants, material properties, substructures, and orientation of the dipole moments. The research on the material

aspects yields important insights about the atomic level sub-phenomena under the domain of main magnetocaloric phenomena. The mathematical study is more equation oriented, in which mathematical techniques are employed to explain the physics of the phenomena. These study methods are valuable in terms of quantification of the variables and developing valid mathematical relations.

3 BOUNDARY CONDITION

The boundary condition of the magnetic field is Ampere's law, which was applied to the regenerator, and the magnetization condition was defined. The magnetization model was applied, and the material was declared as solid; the value of the magnetization defined was 222,000 A/m in the x and y directions, and the values of electrical conductivities and relative permittivity were derived from the material. Magnetic insulation was also applied at the relevant boundaries.

The process modelling and simulation was performed in COMSOL multi physics. The model was drawn in 2D and was inspired by the research performed by the Noume et al., *[7]*, and Hsieh et al., *[9].* The 2D model was drawn in the Comsol model builder geometry, shown in Fig.1

Figure 1*: Comsol 2D model used for the simulation of the magnetocaloric effect*

The length of the fluidic channel is 15.024 cm, while the height of the fluidic channel was kept as 2.5 cm. The magnetic regenerator has been placed at the centre of the channel, and the width and height of the magnetic regenerator were kept as 4.3 cm and 1.5 cm respectively. The right side square box was modelled as a hot heat exchanger, and the left side box was modelled as a cold heat exchanger. The width and height of both heat exchangers are 1.5 and 2.1 cm, respectively.

4 PROPERTIES OF COPPER MATERIAL

The experimental study is based mainly on testing of the magneto-calorific material under different magnetization conditions, equipment development for the measurement of more accurate and fine details, magnetic refrigerator prototype development, and similar. This study involves the sound knowledge of engineering principles.

Table 1: *Show the material properties of the copper in the Comsol*

No.	Material properties off copper			
1	μ	1	[H/m]	Basic
2	ρ	5.998	[S/m]	Basic
3	C	385	J/(kg·K)	Basic
4	e	1	F/m	Basic
5	r	8940	kg/m³	Basic
6	c	400	W/(m·K)	Basic
7	m	1	Pa·s	Basic
8	e	0.5	Ib,w(T)	Basic
9	E	126	Pa	Basic
10	n	0.34	-	Basic
11	r	1.667	Ω·m	Linearized
12	j	3.862	1/K	Linearized
13	T	295.15	K	Linearized

The numerical study is dependent upon the numerical solution of the problem, mainly obtained with the help of computer calculations. The method is useful and beneficial for the parametric design study, and detailed understanding of phenomena. Therefore, the study method adopted in this research is the numerical simulation of magneto-calorific phenomena. The thermodynamic study is mainly dependent upon the heat transfer and thermodynamic analysis of the cycles, systems, and subsystems. The thermodynamic analysis defines the relations for the magnetic field, entropy, and temperature change. It must be mentioned that all study techniques above are usually part of a research publication; however, if the literature is deeply analysed, the research is more inclined towards one of these methods.

The materials were also selected according to the simulations performed by Noume et al., *[7]*, and Hsieh et al. *[9].* The magnetic regenerator placed in the centre was allotted the gadolinium material, the fluid used in the simulation is water, and the plates used to model the heat

exchanger are composed of copper. The material properties of copper used in the simulation, along with COMSOL operators, are shown below.

5 PROPERTIES OF WATER-WORKING AGENT

Table 2: *Properties of water agent in Comsol*

No.	Properties of water-working agent			
1	μ	1	[H/m]	Basic
2	ρ	5.9987	[S/m]	Basic
3	C	385	J/(kg·K)	Basic
4	e	1	F/m	Basic
5	r	8940	kg/m³	Basic
6	c	400	W/(m·K)	Basic
7	m	1	Pa·s	Basic
8	e	0.5	Ib,w(T)	Basic
9	E	126.9	Pa	Basic
10	n	0.34	-	Basic
11	r	1.6678	Ω·m	Linearized
12	j	3.8623	1/K	Linearized
13	T	295.15	K	Linearized

The properties used for gadolinium mostly consist of 3×3 matrices, which are difficult to show here as such. The operators, along with units and properties, are shown below in Table 1.

6 PROPERTIES OF GADOLINIUM MATERIAL

Table 3: *The properties mostly used for gadolinium*

No.	The properties used Gadolinium material	
1	Thermal conductivity	Basic
2	Heat capacity at constant pressure	Basic
3	Electrical conductivity	Basic
4	Density	Basic
5	Relative permittivity	Basic
6	Dynamic viscosity	Basic
7	Resistivity	Basic
8	Coefficient of thermal expansion	Basic
9	Local property HC	Local pr.
10	Local property VP	Local pr.
11	Local property TD	Local pr.
12	Relative permeability	Basic
13	Tangent coefficient of thermal ex.	Thermal
14	Thermal strain	Thermal
15	Isotropic tangent coefficient of ther.	Thermal
16	Isotropic thermal strain	Thermal

The physics selected for the simulations are the main determinants of the solution and boundary conditions. The models used in the simulation are magnetic fields, heat transfer in solids, heat transfer in fluids, and laminar flow for the fluidic solvers. All these have been combined to determine a numerical solution to the magnetocaloric effect problem. COMSOL multi physics excellently combines the physics to formulate a multi physics problem, and the user-friendly interface allows the user to add multiple studies within one window. The proposed multi physics based on different physics selected are also shown in the multi physics tab, and the option is provided to apply it on different domains and boundaries. All the previously defined steps allow the user to define the problem comprehensively.

7 RESULTS

Figure 2 shows the temperature profile. At t=0 sec, the temperature slowly starts dissipating due to the convection effects in the fluid.

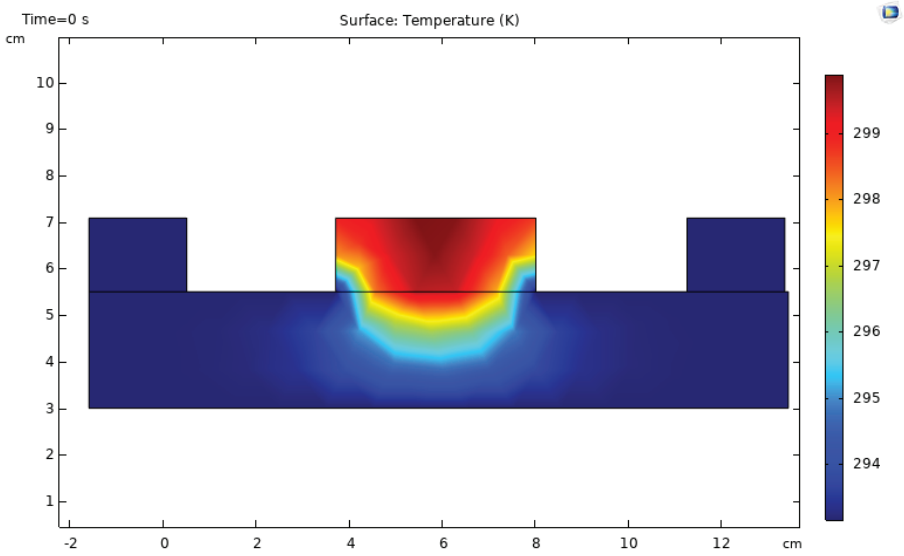

Figure 2: *Temperature of the fluid and the regenerator has been raised*

The values of the temperature are almost the same as that obtained by the Noume et al. in their simulations, *[14].* The temperature rise due to the magnetocaloric effect is similar in magnitude to that has been reported in the literature.

Successful simulations have been performed by using the simplified model techniques and methods. For a more realistic analysis, a transient approach should be adopted. The laminar flow approach has also been adopted in order to reduce the complexity of the solution procedure; otherwise, the flow may be considered turbulent due to heat transfer and fluid flow in the current scenario. The material chosen for the study is widely used in the research of magnetocaloric materials.

8 CONCLUSION

In this article, the process modelling and simulation was performed in Comsol multi physics. The study of gadolinium is focused on the determination of material constants, material properties, substructures and orientation of the dipole moments; the research on the material aspects give important insights about the atomic level sub-phenomena under the domain of main magnetocaloric phenomena. The experimental study is based mainly on-testing of the magneto-caloric material under different magnetization condition equipment, development for the measurement of more accurate and fine details, magnetic refrigerator, prototype development

and similar. This study involves the sound knowledge of engineering principles. The simulation started with the magnetization of the material by using the boundary condition of Ampere's law, which was governed by the magnetic field module. The next step was based on the heat transfer due to the magnetocaloric effect resulting in the temperature rise of the material; the heat begins to transfer into the liquid water, which the final step is based on the flow of the water and resulting in the removal of the heat energy, which is controlled by the laminar flow module.

References

[1] **W. Gao** et al., "Energy transduction ferroic materials", *Materials Today*, vol. 21, no. 7, pp. 771-784, 2018

[2] **V. Franco, J. Blázquez, J. Ipus, J. Law, L. Moreno-Ramírez and A. Conde**, "Magnetocaloric effect: From materials research to refrigeration devices", *Progress in Materials Science*, vol. 93, pp. 112-232, 2018

[3] **A. Smith**, "Who discovered the magnetocaloric effect?", *The European Physical Journal H*, vol. 38, no. 4, pp. 507-517, 2013

[4] **V. Pecharsky and K. Gschneidner Jr**, "Magnetocaloric effect and magnetic refrigeration", *Journal of Magnetism and Magnetic Materials*, vol. 200, no. 1-3, pp. 44-56, 1999

[5] **A. Kitanovski, U. Plaznik, J. Tušek and A. Poredoš**, "New thermodynamic cycles for magnetic refrigeration", *International Journal of Refrigeration*, vol. 37, pp. 28-35, 2014.

[6] **B. Wolf** et al., "Magnetocaloric effect and magnetic cooling near a field-induced quantum-critical point", *Proceedings of the National Academy of Sciences*, vol. 108, no. 17, pp. 6862-6866, 2011

[7] **A. Noume, M. Risser and C. Vasile**, "Modeling of a Magnetocaloric System for Electric Vehicles", in *Comsol Conferrence*, Rotterdam, 2013.

[8] **S. Gombi and D. Sahu**, "Exploration of selected room temperature magneto caloric materials using COMSOL multiphysics", *IOP Conference Series: Materials Science and Engineering*, vol. 577, p. 012160, 2019

[9] **C. Hsieh, Y. Su, C. Lee, P. Cheng and K. Leou**, "Modeling of Graded Active Magnetic Regenerator for Room-Temperature, Energy-Efficient Refrigeration", *IEEE Transactions on Magnetics*, vol. 50, no. 1, pp. 1-4, 2014

Nomenclature

t	time
ρ	density
Q	heat released

JET Journal of Energy Technology

Author instructions

www.fe.um.si/en/jet.html

MAIN TITLE OF THE PAPER
SLOVENIAN TITLE

*Author[1], Author [2], Corresponding author*ℜ

Keywords: (Up to 10 keywords)

Abstract

Abstract should be up to 500 words long, with no pictures, photos, equations, tables, only text.

Povzetek

(Abstract in Slovenian language)

Submission of Manuscripts: All manuscripts must be submitted in English by e-mail to the editorial office at jet@um.si to ensure fast processing. Instructions for authors are also available online at http://www.fe.um.si/en/jet/author-instructions.html.

Preparation of manuscripts: Manuscripts must be typed in English in prescribed journal form (MS Word editor). A MS Word template is available at the Journal Home page.

A title page consists of the main title in the English and Slovenian language; the author(s) name(s) as well as the address, affiliation, E-mail address, telephone and fax numbers of author(s). Corresponding author must be indicated.

Main title: should be centred and written with capital letters (ARIAL bold 18 pt), in first paragraph in English language, in second paragraph in Slovenian language.

Key words: A list of 3 up to 6 key words is essential for indexing purposes. (CALIBRI 10pt)

Abstract: Abstract should be up to 500 words long, with no pictures, photos, equations, tables, - text only.

Povzetek: - Abstract in Slovenian language.

Main text should be structured logically in chapters, sections and sub-sections. Type of letters is Calibri, 10pt, full justified.

ℜ Corresponding author: Title, Name and Surname, Organisation, Department, Address, Tel.: +XXX x xxx xxx, E-mail address: x.x@xxx.xx

[1] Organisation, Department, Address

[2] Organisation, Department, Address

Units and abbreviations: Required are SI units. Abbreviations must be given in text when first mentioned.

Proofreading: The proof will be send by e-mail to the corresponding author in MS Word's Track changes function. Corresponding author is required to make their proof corrections with accepting or rejecting the tracked changes in document and answer all open comments of proof reader. The corresponding author is responsible to introduce corrections of data in the paper. The Editors are not responsible for damage or loss of submitted text. Contributors are advised to keep copies of their texts, illustrations and all other materials.

The statements, opinions and data contained in this publication are solely those of the individual authors and not of the publisher and the Editors. Neither the publisher nor the Editors can accept any legal responsibility for errors that could appear during the process.

Copyright: Submissions of a publication article implies transfer of the copyright from the author(s) to the publisher upon acceptance of the paper. Accepted papers become the permanent property of "Journal of Energy Technology". All articles published in this journal are protected by copyright, which covers the exclusive rights to reproduce and distribute the article as well as all translation rights. No material can be published without written permission of the publisher.

Chapter examples:

1 MAIN CHAPTER

(Arial bold, 12pt, after paragraph 6pt space)

1.1 Section

(Arial bold, 11pt, after paragraph 6pt space)

1.1.1 Sub-section

(Arial bold, 10pt, after paragraph 6pt space)

Example of Equation (lined 2 cm from left margin, equation number in normal brackets (section. equation number), lined right margin, paragraph space 6pt before in after line):

Equation (1.1)

Tables should have a legend that includes the title of the table at the top of the table. Each table should be cited in the text.

Table legend example:

Table 1: *Name of the table (centred, on top of the table)*

Figures and images should be labelled sequentially numbered (Arabic numbers) and cited in the text – Fig.1 or Figure 1. The legend should be below the image, picture, photo or drawing.

Figure legend example:

Figure 1: *Name of the figure (centred, on bottom of figure, photo, or drawing)*

References

[1] **N. Surname:** *Title,* Journal Title, Vol., Iss., p.p., Year of Publication

[2] **N. Surname:** *Title,* Publisher, Year of Publication

[3] **N. Surname:** *Title* [online], Publisher or Journal Title, Vol., Iss., p.p., Year of Publication. Available: website (date accessed)

Examples:

[1] **J. Usenik**: *Mathematical model of the power supply system control*, Journal of Energy Technology, Vol. 2, Iss. 3, p.p. 29 – 46, 2009

[2] **J. J. DiStefano, A.R. Stubberud, I. J. Williams**: *Theory and Problems of Feedback and Control Systems*, McGraw-Hill Book Company, 1987

[3] **T. Žagar, L. Kegel:** *Preparation of National programme for SF and RW management taking into account the possible future evolution of ERDO* [online], Journal of Energy Technology, Vol. 9, Iss. 1, p.p. 39 – 50, 2016. Available: http://www.fe.um.si/images/jet /Volume 9_Issue1/03-JET_marec_2016-PREPARATION_OF_NATIONAL.pdf (7. 10. 2016)

Example of reference-1 citation: In text *[1],* text continue.

Nomenclature

(Symbols)	(Symbol meaning)
t	time

JET

JET I Journal of Energy Technology I Vol. 13, Issue 2, September 2020 I University of Maribor, Faculty of Energy Technology

ISSN 1855-5748

9 771855 574008